Draft Manuscript for Review

Using Zircon Isotope Compositions to Constrain Crustal Structure and Pluton Evolution: The Iapetus Suture Zone Granites in Northern Britain

Journal:	*Journal of Petrology*
Manuscript ID:	JPET-Dec-12-0134.R2
Manuscript Type:	Original Manuscript
Date Submitted by the Author:	07-Oct-2013
Complete List of Authors:	Miles, Andrew; University of Edinburgh, School of GeoSciences Graham, Coliin; University of Edinburgh, GeoSciecnes Hawkesworth, Christopher; University of St. Andrews, School of Geography and Geosciences Gillespie, Martin; British Geological Survey, Dhuime, Bruno; University of Bristol, Dept. of Earth Sciences Hinton, Richard; University of Edinburgh, School of Geosciences
Keyword:	zircon, granite, isotope, Iapetus Suture

Using Zircon Isotope Compositions to Constrain Crustal Structure and Pluton Evolution: The Iapetus Suture Zone Granites in Northern Britain

Andrew Miles[a,*], Colin Graham[a], Chris Hawkesworth[b], Martin Gillespie[c], Bruno Dhuime[b,d] and Richard Hinton[a]

[a]*School of GeoSciences, King's Buildings, West Mains Road, University of Edinburgh Edinburgh, EH9 3JW, UK*

[b]*School of Geography and Geosciences, University of St Andrews, North Street, St Andrews, KY16 9AL, UK*

[c]*British Geological Survey Murchison House, West Mains Road, Edinburgh, EH9 3LA, UK*

[d]*Department of Earth Sciences, University of Bristol, Wills Memorial Building, Queen's Road, Bristol BS8, 1RJ, UK*

**Corresponding author current address: School of Geography, Geology and the Environment, Kingston University, Penrhyn Road, Kingston upon Thames, Surrey, KT1 2EE, UK. Telephone +44 (0) 131 650 5916. E-mail: Andrew.Miles@kingston.ac.uk*

ABSTRACT

The Trans-Suture Suite (TSS) of calc-alkaline granite plutons straddle both sides of the Iapetus Suture in Northern Britain. Their emplacement during the early Devonian post-dates subduction of the Iapetus Ocean and their origin and tectonic relations have proved difficult to reconcile with tectonic evidence for orogenic convergence and uplift. We report the first *in-situ* study of zircon U-Pb, O and Hf isotopes from magmatic zircons from three TSS granites. Ages of 410 ± 6 Ma for the Criffell pluton, 416 ± 5 Ma for the Shap pluton and 410 ± 3 Ma for the outer zone of the Fleet pluton are coincident with the intrusion of regionally prolific lamprophyre dykes within transtensional tectonic environments. Resolvable age differences between the outer and inner two zones of the Fleet pluton (387 ± 5 Ma) suggest two distinct stages of emplacement that bracket a ~ 10 Myr phase of transpression recognised from geological evidence. Mean zircon oxygen isotope compositions ($\delta^{18}O$) range from ~ 5.0 ‰ up to ~9.0 ‰ and generally increase in tandem with inter-grain isotope heterogeneity in more silicic magmas, providing evidence for increased additions from sedimentary sources in addition to the involvement of more mafic magmas. Magmatic zircons from dioritic enclaves from the Criffell granodiorites have U-Pb ages up to ~ 9 Myr older than their host rocks and have distinct oxygen isotope population distributions. It is suggested that these may represent entrained, cognate material derived from deeper crustal hot zones. Initial εHf values from the three plutons are distinct from each other, show little or no variation within plutons and differ substantially from mantle values, requiring significant crustal re-working. Zircon Hf model ages (0.9 to 1.0 Ga) indicate that most re-worked crust was of Avalonian origin, consistent with geophysical evidence for underlying Avalonian crust beneath the Iapetus Suture.

KEY WORDS: Iapetus Suture; Isotopes; Granite; Zircon

INTRODUCTION

Granite plutons are amongst the most characteristic manifestation of the processes of partial melting and magmatic differentiation that ultimately determine the evolution of large proportions of the continental crust (Campbell & Taylor, 1983; Kemp *et al*. 2007). The contrasted isotopic compositions of granitic rocks and the mantle (Appleby *et al*. 2008; DePaolo 1981; Gray 1984; Hamilton *et al*. 1980; Jahn *et al*. 2000; Keay *et al*. 1997; Kemp *et al*. 2007; McCulloch & Chappell, 1982; Chappell and White, 1974) reflect the variable involvement of reworked crustal material in their formation that is additional to – or exclusive of - the effects of direct fractionation of mantle-derived magmas. The isotopic compositions of granitic rocks therefore frequently serve as windows into the chemical evolution and lithological configuration of their source regions.

Extensive whole-rock trace element and isotopic work has been directed towards identifying the sources of magmas through time on the continental margin of the evolving British Caladonides, and has revealed regional variations in the continental crust and lithospheric mantle (e.g. Canning *et al*. 1996; Thirlwall, 1989; Frost & O'Nions, 1985; Halliday, 1984; Stephens and Halliday, 1984; Halliday *et al*. 1980; Hamilton *et al*. 1980; Harmon & Halliday, 1980; Pidgeon & Aftalion, 1978). These studies have enabled distinct crustal terranes to be identified throughout Northern Britain, with important regional implications for the tectonic reconstruction of the Caledonides.

Whole-rock studies have also identified a distinct sub-set of Devonian (post Caledonian) plutons in Northern Britain that straddle the Iapetus Suture - the former tectonic boundary between the continents of Avalonia and Laurentia - and are referred to as the Trans-Suture Suite (TSS) of granites (Brown *et al*. 2008). Their positioning across the Iapetus Suture Zone precludes a simple subduction origin (Soper, 1986; Thirlwall, 1981). Furthermore, their mutual compositional similarities raise the possibility of a common source region on both sides of the suture zone beneath the English Lake District and Scottish Southern Uplands (Halliday, 1984; Harmon & Halliday, 1980; Harmon *et al*. 1984; Highton, 1999; Stephens, 1988; Thirlwall, 1989). A further unusual feature of the granites is the absence of inherited zircons despite the occurrence of large volumes of granitic rocks with S-type and peraluminous characteristics (Pidgeon & Aftalion, 1978; Miles *et al.* 2013) that require a major input from sedimentary sources.

Whole-rock compositions provide only cumulative evidence for the complex processes that ultimately determine magma compositions and are also subject to later, post-solidus alteration. For example, mafic enclaves found in a number of plutons within the TSS potentially reflect the interaction of variably silicic magmas, but the origin of these enclaves has proved difficult to constrain from whole-rock studies alone (see Holden *et al.* 1987). However robust accessory minerals such as zircon that preserve chemical evidence for the stable and radiogenic isotope compositions of their host magmas at the time of crystallisation may now be analysed to circumvent these problems to reveal different magmatic processes at high temporal and spatial resolution (e.g. Appleby *et al*. 2008, 2010; Bradley, 2011; Griffin *et al.* 2002; Hawkesworth & Kemp, 2006; Kemp *et al*. 2007; Kinny & Maas, 2003; Roberts 2012;

Valley *et al*. 2005). Improvements in the micro-analysis of accessory minerals now enable high precision, high spatial resolution *in situ* analyses of zircon isotope compositions to be integrated with U-Pb dating (Ireland & Williams, 2003; Parrish and Noble, 2003) in order to reveal a detailed record of magma sources and their evolution.

In this study, high precision and spatial resolution micro-analytical isotope techniques are applied to provide a revised geochronological framework to determine the chronology and test the synchronicity of the TSS of plutons in relation to the regional geological and tectonic evolution. Within this framework, the oxygen and hafnium isotope compositions of magmatic zircons are used to characterise the different source components in the lower crust and upper mantle and to relate these to independent geological, geochemical and geophysical evidence.

GEOLOGICAL BACKGROUND

The Caledonian Orogeny and Tectonic Evolution of the Iapetus Suture Zone

The Caledonian Orogeny had a protracted and complex history throughout the early Paleozoic up to the early Devonian that resulted in the destruction of the Iapetus Ocean that once separated the former continents of Laurentia and Avalonia. The earliest orogenic events in Scotland were associated with closure of a back-arc basin and collision of the continent-facing Midland Valley arc (Bluck, 1983) with the Laurentian margin to the northwest during the Grampian Orogeny (470-460 Ma). Southward subduction of oceanic crust ceased following arc collision, and subsequent northward-directed subduction beneath the accreted arc marked the onset of Iapetus closure due to subduction beneath Laurentia (Leggett *et al*. 1983). Northward subduction was associated with propagation of the Southern Uplands–Longford Down accretionary prism in the hanging wall of the suture zone (Barnes *et al*. 1989). On the adjacent Avalonian margin, final closure of the Iapetus Ocean was signalled by deposition of the Windermere Supergroup (late Ordovician to end Silurian in age) within an associated flexural basin (Kneller, 1991). Reduced accretionary deformation in the sediments of the Southern Uplands accretionary prism, dated using graptolite biostratigraphy, is evident during the late Wenlock period (422 - 428 Ma), signalling a slowing of Iapetus subduction (Kemp, 1987). The emplacement of minor K-lamprophyre dykes in the Southern Uplands also spans the final stages of accretionary deformation and includes a suite of older foliated and younger unfoliated dykes. The unfoliated dykes give Rb-Sr isochron and K-Ar ages in the range of 400 – 418 Ma (Rock *et al*. 1986) and suggest that convergence and deformation had stopped by 418 Ma. Together, biostratigraphic and geochronological evidence suggest that convergence ceased by *c*. 420 Ma. Subsequently, the formation of extensive Old Red Sandstone basins, the emplacement of regionally prolific lamprophyre dykes together with multiple clockwise-transecting cleavages in many basins throughout Northern Britain during the Early Devonian suggests a transition to alternating phases of transtension and transpression during oblique convergence of Laurentia and Avalonia (Dewey & Strachan, 2003; Soper & Woodcock, 2003). Later regional folding, faulting and cleavage formation are evident, particularly in the Lake District, towards the early Devonian. The coeval nature of this deformation with the Acadian Orogeny in the Canadian Appalachians led Soper (1987) to refer to this as the Acadian Event in Britain, which has been linked to further compression of Eastern Avalonia and Laurentia caused by collision of the Armorica microcontinent (Soper 1986; Soper *et al*. 1992).

Post-Caledonian Magmatism across Northern Britain

Despite the above biostratigraphical and geochronological evidence that subduction of the Iapetus Ocean had ceased by *c.* 420 Ma, plutonic and volcanic calc-alkaline magmatism with subduction-like geochemical characteristics then became prevalent, particularly on the Laurentian terrane, and continued until the early Devonian. The igneous rocks have particularly high K_2O, Mg, Ni, Cr and V contents, are mainly silica-saturated, and have been attributed to the mixing of primitive mantle melts with sediments thought to be subducted lower Palaeozoic greywackes (Thirlwall, 1982, 1983, 1986). Broad, systematic variations in the compositions of igneous rocks were found perpendicular to the main Caledonian structural trends (Thirlwall, 1981; Stephens & Halliday, 1984). These variations were considered to be consistent with a WNW-dipping subduction zone beneath Scotland, where the depth of melting increased away from the Iapetus Suture Zone (Thirlwall, 1982), but are difficult to reconcile with geological evidence that Iapetus subduction had ceased by *c.* 420 Ma (Brown *et al*. 2008).

A number of alternative tectonic models have been proposed to reconcile apparently conflicting evidence. These include volatile loss from a stationary slab (similar to the Cascades of California and Oregon; Thirlwall, 1981) and fluxing of the overlying mantle wedge by active subduction followed by later shearing, extension and mantle melting (Hutton & Reavy, 1992). Freeman *et al*. (1988) suggested that the Avalonian subcontinental mantle became detached from its overlying crust and continued to subduct, while others have proposed slab break-off following orogenic thickening to account for voluminous metaluminous magmatism and rapid uplift

(Atherton and Ghani, 2002; Oliver *et al*. 2008; Neilson *et al*. 2009; Cooper *et al.* 2013). The latter authors suggested that slab break-off resulted in asthenospheric upwelling and melting of the subcontinental lithosphere to form a lamprophyric underplate that subsequently led to the remelting of the lower crust through thermal advection and conduction. O'Reilly *et al.* (2012) suggested that changes in the distribution of vertical stresses within the crustal and mantle parts of the subucting lithosphere led to a concentration of stress in the brittle mantle below the Moho, termed 'incipient delamination'. They proposed that tensile cracks formed which were intruded by mafic magmas from partial melting within the subducting lithosphere and, or, surrounding asthenosphere, increasing the heat flux into the surrounding crust and, triggering silicic magma generation. These models invoke a genetic link between the regional occurrence of lamprophyric magmas and apparently much larger volumes of calc-alkaline plutonic and volcanic material.

The plutonic and volcanic rocks that straddle the Iapetus Suture have proved particularly difficult to reconcile with any of the regional tectonic models discussed previously. For example, the emplacement of some plutons south of the suture in areas such as the English Lake District, the Pennines, the Isle of Man and Eastern Ireland (Brown *et al*. 2008) preclude models that invoke volatile loss from a stationary slab or active subduction. Crustal delamination beneath the Southern Uplands following lithospheric thickening also seem unlikely because of the low metamorphic grade (prehnite-pumpellyite facies) of local sedimentary rocks (Kemp, 1987) that in turn indicate only modest crustal thickening. Furthermore, magmatism in response to slab break-off is again difficult to reconcile with the intrusion of some plutons south of the suture zone. Brown *et al*. (2008) proposed a transtensional model for the formation of the TSS, drawing particular attention to the coeval deposition of the Old Red Sandstone sediments in apparently transtensional basins during the early Devonian on both sides of the suture zone. Their deposition has been shown to require tectonic subsidence linked to enhanced geothermal gradients in the Welsh slate belts due to extension and passive mantle upwelling (Soper & Woodcock, 2003). Extension or transtension is also consistent with the concurrent intrusion of the SW-NE trending regional K-lamprophyre dykes formed following small amounts of lithospheric thinning and adiabatic mantle melting between 420 Ma and 400 Ma (Brown *et al*. 2008; Dewey & Strachan, 2003; Rock *et al*. 1986). However, Brown *et al*. (2008) acknowledge that published ages for the TSS suggest emplacement during periods when independent sedimentary and tectonic evidence is indicative of transpression.

The Trans-Suture Suite (TSS) granites

The predominantly metaluminous, post-Caledonian Devonian Scottish granites were distinguished from the older peraluminous granites found in northern Scotland by Read (1961), while further subdivisions based primarily on isotopic differences have been shown to reflect the influence of different crustal terranes (Stephens & Halliday, 1984; Stone & Evans, 1997). Furthermore, the Criffell and Fleet plutons of Southern Scotland have been shown to share many compositional characteristics (e.g. $^{207}Pb/^{204}Pb$) with plutons of similar age in the English Lake District such as Shap, emplaced within Avalonian crust (Harmon & Halliday, 1980; Harmon *et al*. 1984; Highton, 1999; Stephens 1988; Thirlwall, 1989). These and related plutons have been grouped by Brown *et al.* (2008) and collectively referred to as the Trans-Suture Suite (TSS).

U-Pb dating has consistently shown that plutons emplaced south of the Highland Boundary Fault lack inherited zircon and provide only emplacement ages (Pidgeon and Aftallion, 1978 and this study). By contrast, plutons north of the Highland Boundary Fault commonly contain a significant proportion of inherited zircons, many with Archean ages consistent with underlying basement of a similar age. Pidgeon & Aftalion (1978) attributed these differences to an absence of older basement material south of the Highland Boundary Fault but this absence may also reflect resorption during magma ascent (Miles *et al*. 2013).

The Criffell Pluton

A Rb-Sr isochron age suggests that the Criffell pluton was emplaced at ~397 ± 2 Ma (Halliday *et al*. 1980) into low-grade wackes and pelites of Llandovery to Wenlock age that form part of the Southern Uplands accretionary prism in southern Scotland (Fig. 2a). The pluton is of historical significance as a classic example of a normally zoned pluton (Stephens & Halliday 1980; Stephens *et al*. 1985). Outer zones (1 and 2) are of metaluminous granodiorite (~ 59 to 69 wt % SiO_2, Fig. 3) containing primary hornblende (with occasional cores of clinopyroxene), biotite, zoned plagioclase, potassium feldspar, quartz and accessory titanite, zircon, apatite and magnetite (with very minor hematite) (Figs. 4 and 5). Inner zones (4 and 5) are composed of peraluminous granite (~ 69 to 73 wt % SiO_2, Fig. 3) and contain primary muscovite but lack hornblende, titanite and the abundant zircon and magnetite that characterise the granodiorites. Insufficient zircon was found in samples from Zone 5 and we therefore focus our study on samples from zones 1 to 4.

Mineralogical zoning is accompanied by isotopic zoning, with outer granodiorites having initial $^{87}Sr/^{86}Sr$ ratios of 0.7052 (Halliday *et al*. 1980), εNd values of -0.6 (Halliday, 1984) and $\delta^{18}O$ values of 8.5 ‰ (Halliday *et al*. 1980). Inner granites have initial $^{87}Sr/^{86}Sr$ ratios up to 0.7073, εNd values of -3.1 and $\delta^{18}O$ values of 11.9 ‰. Simultaneous variations in isotope and Rare Earth Element (REE) compositions were interpreted by Stephens *et al*. (1985) to result from assimilation and fractional crystallisation (AFC) involving both mafic lower crustal/mantle and sedimentary components. The absence of local melting in the surrounding country rocks indicates that immediately adjacent sediments were not a major source of contamination, while the Pb isotope compositions of the TSS are markedly different from that of the Southern Uplands sediments (Thirlwall, 1989).

Mafic enclaves are a common feature in the outer three zones of the pluton. Oscillatory zoned plagioclase within the enclaves provides evidence for a magmatic origin (Holden *et al*. 1987). The enclaves have been variously interpreted to represent residual components following partial melting of the crust, restite from a basic precursor, cognate material, congealed syn-plutonic injections of basic magma or segregated immiscible liquids (see Holden *et al*. 1987).

The Fleet Pluton

The ~ 10 km by 12 km Fleet pluton intrudes the Llandovery sediments (428 to 444 Ma) of the Central Belt of the Southern Uplands (Fig. 2b) and is situated south of the Orlock Bridge fault (Fig. 1). Pidgeon & Aftalion (1978) reported a zircon U-Pb age of 396 ± 6 Ma from near the margin of the granite, within error of a Rb-Sr mineral-whole-rock isochron age of 392 ± 2 Ma (Halliday *et al*. 1980). A foliation related to ductile deformation wraps around cordierite porphyroblasts in the aureole and is cut by the granite contact. This has been suggested to reflect syn-tectonic emplacement of the pluton during reactivation of the Moniaive Shear Zone caused by Acadian deformation (Lintern *et al*. 1992; Phillips *et al*. 1995; Barnes *et al*. 1995; Brown *et al*. 2008; Stone & Evans, 1997). Gravity anomalies indicate that the pluton extends to a depth of ~ 11 km beneath the current surface (Parslow & Randall, 1973). SiO_2 contents vary from 69 to 76 wt% and are on average more evolved than other TSS granites. Their typical peraluminous compositions (Fig. 3) are reflected in their petrology: the pluton has two main granite facies, including an outer biotite granite and inner biotite-muscovite granite (Figs. 2 and 4). The latter facies has subsequently been subdivided into fine and coarse grained units (Parslow, 1968).

Elevated initial $^{87}Sr/^{86}Sr$ ratios of 0.7062 to 0.7083 and low εNd values of -3.0 to -3.4 (Stephens & Halliday, 1984) also reflect the predominantly peraluminous character of the Fleet pluton, with evolved whole-rock $\delta^{18}O$ values of ~11‰ indicative of a large sedimentary component (Halliday, 1984; Halliday *et al*. 1980; Stephens & Halliday, 1984). The Fleet pluton has been shown to share many geochemical similarities with the Lake District plutons (Stephens & Halliday, 1984; Thirlwall, 1989), post-dating closure of the Iapetus Ocean.

The Shap Pluton

The Shap pluton was emplaced into Caradoc (~ 455Ma) volcanic rocks of the Borrowdale Volcanic Group (BVG) in the English Lake District (Figs. 1 and 2c). Pidgeon & Aftalion (1978) reported a zircon U-Pb age of 390 ± 6 Ma, while Wadge (1978) reported an age of 394 ± 3 Ma based on a whole-rock-feldspar Rb-Sr isochron, similar to the 397 ± 7 Ma age estimated from K-Ar biotite dating. Davidson *et al*. (2005) reported an older plagioclase-rimmed K-feldspar Sr isochron age of 405 ± 2 Ma.

Stephenson (1999) noted three distinct stages of pluton growth based primarily on the modal abundance of large K-feldspar megacrysts now thought to be igneous in origin (Lee *et al*., 1995). Stage 1 (~10% volume of the pluton) is represented by the outer margins of the pluton with 15% pink, Carlsbad-twinned orthoclase-perthite megacrysts up to 5 cm in size. The groundmass consists of orthoclase, plagioclase (zoned from andesine to albite), quartz and biotite (Fig. 4). Accessory minerals include titanite, apatite, magnetite, zircon, fluorite, monazite, allanite, amphibole and pyrite. The dominant stage 2 granite (90% of the pluton) is broadly similar to the stage 1 granite but contains 30% orthoclase and reduced proportions of biotite. This trend continues into the final (stage 3) granitic veins with up to 60% orthoclase megacrysts.

Significant assimilation of sediments is indicated by elevated ^{18}O compositions, with $\delta^{18}O$ values of ~11‰, initial $^{87}Sr/^{86}Sr$ values (0.707) and low εNd (-2.0) (Wadge et 1978; Harmon & Halliday, 1980; Halliday, 1984). However, the predominantly metaluminous mineralogy of the Shap granite raises the possibility that crustal fluids have significantly altered the isotopic composition of the pluton either during or post emplacement (Halliday, 1984). Hydrothermal processes are also implied by the presence of fluorite and pyrite.

Abundant megacryst-bearing microdioritic inclusions up to 2m in size occur in addition to country rock xenoliths in the Shap pluton. Many authors have suggested that such features represent injections of mafic magma, possibly related to the intrusion of a regional K-lamprophyre dyke swarm (Granthem, 1928; Stephenson, 1999; Cox *et al*. 1996).

In summary, published data indicate that all three TSS plutons were intruded at similar times between 397 Ma and 390 Ma during a period dominated by transpression (Brown *et al*. 2008), and share many common chemical characteristics, including elevated initial $^{87}Sr/^{86}Sr$ and similar $^{207}Pb/^{204}Pb$ isotope compositions that resemble Skiddaw Group sedimentary rocks found in the English Lake District within the Avalonian terrane. The Criffell and Fleet plutons are chemically and mineralogically zoned, both characterised by more evolved core zones and more primitive outer zones. The plutons differ mainly in their major element compositions and in the scale of chemical zoning. The Criffell pluton is zoned from a metaluminous outer region to a more peraluminous inner region (Fig. 3), while the Fleet pluton is entirely peraluminous, and becomes increasingly peraluminous towards its inner zones.

Present-day Structural and Lithological Distribution of the Iapetus Suture

Evidence from seismic profiles constrains crustal structure and lithological components across the Iapetus Suture and northwards through the Caledonian fold belts of northern Britain. Northwest-southeast seismic profiles from the BIRPS seismic survey have imaged a north-dipping (~ 20^{o}) zone of reflectivity in the middle and lower crust traced over 900 km from the Atlantic margin west of Ireland to the North Sea (Beamish & Smythe, 1986; Freeman *et al*. 1988; Hall *et al.* 1984; Klemperer & Matthews, 1987; Klemperer *et al*. 1991). This reflection is interpreted to represent Avalonian crust underthrust beneath the Laurentian margin. Brown *et al*. (2008) suggest that flattening of subducting Iapetus oceanic lithosphere occurred in response to the subduction of progressively younger and more buoyant lithosphere up to 420 Ma. The geometry of the suture zone close to the Moho is less certain, but it appears to flatten and merge with a set of strong sub-horizontal reflections in the lower crust beneath the Midland Valley, interpreted as Iapetus oceanic crust or imbricated basement and sedimentary cover from the continent-ocean margin of Avalonia (Soper *et al*. 1992). These reflectors indicate that underthrust Avalonian crust extends at least as far north as the Midland Valley and supports isotopic evidence for the presence of Avalonian sediments (similar to the Skiddaw Group found in the English Lake District) in the formation of plutons situated on the Laurentian terrane in Southern Scotland (Thirlwall, 1989).

Here we use the U-Pb, O and Hf isotope compositions of zircons from the TSS and an understanding of the structural and lithological make-up of the crust to identify the source lithologies that contribute to the TSS granites and provide a new geochronological timeframe for their emplacement.

METHODOLOGY

Zircon preparation

Rock samples of approximately 5 kg from different zones of the Criffell, Fleet and Shap plutons were crushed and sieved to < 500 μm prior to density separation using a

Wilfley Table at the University of St Andrews separation facility. Heavy liquids, including Tetrabromoethane (TBE) and methylene iodide, were used for further mineral separation. Non-magnetic fractions were separated using Frantz magnetic separators at the Universities of St Andrews and Edinburgh. Approximately 100 zircon crystals were picked from each sample and mounted in epoxy (Araldite/Epothin) blocks with fragments of 91500 zircon standard positioned at the centre of each block. Polished mounts were imaged by back-scattered electron (BSE) and cathodoluminescence (CL) imaging using a Phillips XL30CP Scanning Electron Microscope (SEM) at the University of Edinburgh to establish the positions of inclusions, cracks and internal compositional zoning (Fig. 5). Oxygen isotope, trace element and U-Pb analyses of zircons were carried out (often on the same grains) using Secondary Ionisation Mass Spectrometry (SIMS) at the University of Edinburgh. Oxygen analyses were carried out prior to U-Pb dating in order to avoid implantation by the ^{16}O beam used for U and Pb isotope analysis. Hf isotope compositions were determined last (due to the large, 40 – 60 µm beam size) by inductively-coupled plasma mass spectrometry (ICP-MS) at the University of Bristol. Hf isotope compositions were frequently determined using the same grains used for other chemical analyses and consequently, laser pits often obscure earlier SIMS analytical spots. Samples were cleaned but not polished between analyses on different instruments.

Zircon U-Th-Pb analysis

U-Th-Pb dating was carried out following oxygen isotope analysis using a Cameca ims 1270 ion microprobe at the University of Edinburgh. A 4 to 5 nA primary O^{2-} beam was used for zircon analysis with 22.5 keV impact energy following the method of Kelly *et al*. (2008). Resulting analytical pits were ~ 25 μm and ellipsoidal in shape following beam focusing and alignment under Köhler illumination, with further spatial resolution achieved using a field aperture. U, Th and Pb were analysed at a mass resolution (M/ΔM) of > 4000R using a peak switching routine. No energy centring was carried out and an energy window of 60 eV was used throughout. Pb ion yields were increased by a factor of ~ 2 by flooding the sample surface with oxygen. Any effects from surface contamination were minimised by pre-rastering a ~ 15 μm surface area for 120 seconds prior to analysis. Pb/U ratios were calibrated using a slope factor of 2.6 between ln (Pb/U) vs. ln (UO_2/U). U/Pb ratios were calibrated against measured ratios of zircon standard 91500 with an age of ~1062.5 Ma and assuming a $^{206}Pb/^{238}U$ ratio of 0.17917 (Wiedenbeck *et al.* 1995). Standard analyses were carried out after every 3 to 4 unknown analyses. Calculated Th/U ratios in all unknown samples were obtained by comparison with measured Th/U ratios (Th/U = 0.362) and $^{206}Pb/^{238}U$ in zircon standard 91500 assuming closed system behaviour. U and Hf concentrations of 81.2 ppm and 5880 ppm respectively in the standard were assumed and elemental concentrations determined based on the observed oxide ratios of the standard (UO_2/Zr_2O_2 and HfO/Zr_2O_2).

Corrections for dead time (51 ns), detector background (~ 0.01-0.03 counts per second) and common Pb (^{204}Pb) were conducted. Pb corrections were carried out using present day ^{204}Pb and the following ratios: $^{206}Pb/^{204}Pb$ = 18.70, $^{207}Pb/^{204}Pb$ = 15.63 and $^{208}Pb/^{204}Pb$ = 38.63. Measurements with ^{204}Pb > 10 ppb were discarded because of large common Pb corrections. Uncertainties in the U/Pb ratio of 91500 are approximately 0.8 % greater than those expected from counting statistics alone and are assumed to be random errors (Ireland & Williams, 2003). These random errors have been propagated (in standards and unknowns) together with the observed variations in Pb/U ratios measured for each analysis (typically close to the counting errors). Measurements carried out on zircon Geostandard 91500 are typically between 0.7 and 1.0 % per analysis. Observed variations in $^{207}Pb/^{206}Pb$ ratios from cycle to cycle during each analysis approach those expected from counting statistics. Quoted uncertainties on individual ages are 1 SD while those on calculated group ages are quoted as 2 SD.

ISOPLOT (version 3) was used for plots and age calculation (Ludwig 2003), with mean and weighted mean $^{206}Pb/^{238}U$ concordant ages used for magmatic zircons. BSE and SE imaging of analytical pits were subsequently used to assess pit quality, cracks and the presence of inclusions.

Replicate U-Pb analyses were not possible in most cases due to limited fresh surfaces on many crystals.

Zircon oxygen isotope analysis

Oxygen isotope analysis of zircons was carried out using a Cameca ims 1270 ion microprobe at the University of Edinburgh following the methods described by Cavosie *et al*. (2005) and Kemp *et al*. (2006b), with data reported as per mil (‰) values relative to Vienna Standard Mean Ocean Water (VSMOW). A primary $^{133}Cs^{+}$ ion beam of approximately 20 µm diameter was used at 6 nA. A normal-incidence electron flood gun was used for charge neutralisation, with secondary ions extracted at 10 kV. Both $^{18}O^{-}$ and $^{16}O^{-}$ ions were monitored simultaneously on dual Faraday cups. Total acquisition times of ~ 200 seconds included secondary ion beam centring, presputtering for 50 seconds and data collection over 10 cycles, each lasting 4 seconds. Instrumental drift was corrected daily by normalising all unknown samples to zircon standard 91500 ($\delta^{18}O$ = 9.86 ‰) (Wiedenbeck *et al*. 2004). Bracketing analyses of 91500 were used to obtain linearly interpolated values of $^{18}O/^{16}O$ that were subsequently used to normalise the $^{18}O/^{16}O$ ratios of unknown samples. Analyses of 91500 in groups of 5 to 10 were carried out after every 10 to 15 analyses of unknowns. Following corrections for instrument drift, unknown zircon analyses were normalised to an average daily $^{18}O/^{16}O$ value for zircon standard 91500.

HfO_2 concentrations in unknown zircon samples were determined using Cameca SX100 electron microprobes at the Universities of Edinburgh and Bristol. Variations in the instrumental mass fractionation (IMF) during $^{18}O/^{16}O$ analysis by ion microprobe have been shown to reflect variations in HfO_2, particularly analyses at high energy offset using a Cameca ims 4f (Peck *et al*. 2001). IMF corrections were not required in this study due to the use of a Cameca ims 1270 (which does not require high energy offset) and the small measured variations in HfO_2 (generally < 0.5 wt%). Zircon oxygen isotope data are presented as histograms with bin widths determined from 1 SD precision in the $\delta^{18}O$ composition of 91500. Cumulative probability curves are fitted by summing the probability distributions of a suite of data with normally distributed errors (Isoplot ver. 3.00; Ludwig, 2003). Grain-scale variation plots illustrate the extent to which data lie within analytical error (2 SD) of the mean.

Following the approach of Appleby *et al*. (2008), zircon standard 91500 is assumed to have a homogenous isotopic composition. Variations greater than 2σ about the mean δ^{18}O of 91500 are considered to be real. Analytical precision from session to session was generally between 0.3 and 0.6 ‰.

Zircon Hf isotope analysis

Zircon Lu-Hf isotope compositions were obtained using a ThermoFinnigan Neptune multicollector inductively-coupled plasma mass spectrometer (MC-ICP-MS) coupled with a New Wave Research UP193HE laser at the University of Bristol. Similar sites to those used for oxygen isotope analyses were chosen using a spot size of 40 or 50 μm. Ablation was carried out in helium and later mixed with argon and nitrogen using a pulsed laser at 4 Hz with an energy density of ~ 6 J/cm^2 over 60s. Total analysis times were ~ 90s, including 30s of background measurements. Corrections for interferences and mass bias followed the University of Bristol procedure outlined by Hawkesworth & Kemp (2006). Mass bias effects with interference-free ^{171}Yb were corrected using an exponential law and ^{173}Yb/^{171}Yb = 1.130172 (Segal *et al*. 2003). A ^{176}Yb/^{171}Yb value of 0.897145 was used to calculate the ^{176}Yb interference on ^{176}Hf (Segal *et al*. 2003) with mass bias-corrected ^{171}Yb monitored during the run. Mass bias effects on interference-free ^{175}Lu were conducted assuming βLu = βYb and using an exponential law. Mass bias-corrected ^{176}Lu was monitored during the run and the magnitude of the ^{176}Lu interference on ^{176}Hf was calculated using ^{176}Lu/^{175}Lu = 0.02655 (Vervoort *et al*. 2004). An exponential law was used to correct for mass bias on interference corrected ^{176}Hf/^{177}Hf values before normalising to Hf standard JMC-475 = 0.282160. The accuracy and long term reproducibility of the measurements was estimated by analysing two zircon reference standards, including Plesovice (^{176}Hf/^{177}Hf = 0.282476 (25), *n = 29* with a 40μm beam; ^{176}Hf/^{177}Hf = 0.282474 (17), *n = 36* with a 50 μm beam) and Mud Tank (^{176}Hf/^{177}Hf = 0.282503 (27), *n = 27* with a 40µm beam; $^{176}Hf/^{177}Hf$ = 0.282501 (18), *n = 30* with a 50µm beam) (errors are reported at 2 SD). The average $^{176}Hf/^{177}Hf$ compositions of both standards were within error of accepted values (Plesovice: $^{176}Hf/^{177}H$ = 0.282482 ± 0.000013, Sláma *et al*. 2008); Mud Tank: $^{176}Hf/^{177}Hf$ = 0.282507 ± 0.000006, Woodhead and Hergy, 2005)). Initial εHf values for all samples were calculated using the mean $^{206}Pb/^{238}U$ ages for each zone. Epsilon values are reported relative to initial Chondritic Uniform Reservoir (CHUR) values calculated from present day values of $^{176}Lu/^{177}Hf$ = 0.0336 and $^{176}Hf/^{177}Hf$ = 0.282785 (Bouvier *et al*. 2008). A ^{176}Lu decay constant of $\lambda = 1.867 \times 10^{-11}$ yr^{-1} (Scherer *et al*. 2001) was used.

RESULTS

A summary of the zircon O-Hf-U-Pb isotope compositions for each zone of the Criffell, Fleet and Shap plutons together with associated enclaves is provided in Table 1 and illustrated in Figs 6-9. Variations in O, Hf and U-Pb isotope values are generally limited within single zones and are therefore presented as mean values. Small crystals, cracks and inclusions limited multiple analyses on single grains. Errors represent 2 SD variations about the mean values. Sample labelling includes the sample number, subscript and grain number.

The Criffell Pluton

Zircons from all zones have a mean $^{206}Pb/^{238}U$ age of 410 ± 6 Ma (*n* = 29) (Table 1). A large number of zircons from all zones have crystallisation ages that lie within analytical error of each other, includes in regions with and without oscillatory zoning. One analysis from Zone 1 yielded an anomalously young age of 394 ± 4 Ma (1SD analytical error). While this may represent a real age difference, this grain is also characterised by high ^{204}Pb (3.12 ppb) relative to other grains with older ages and may therefore not be as accurate.

Mean zircon oxygen isotope compositions (Fig. 7) and heterogeneity amongst populations increase towards more inner zones: Zone 1 (5.8 ± 0.8 ‰ (2SD; n = 13), Zone 2 (5.9 ± 0.9 ‰ (2SD; n = 13), Zone 3 (6.5 ± 1.0 ‰ (2SD; n = 21), Zone 4 (7.2 ± 1.4 ‰ (2SD; n = 28). In zones 1, 2 and 3, 70%, 80% and 90% respectively of grains lie within analytical error of their population means (calculated independently for each session). By comparison, only 64% of analyses in zone 4 lie within analytical error of the population mean.

Zircon εHf_t compositions show limited variation and range between + 2.3 and + 4.4. Mean εHf_t values for each zone largely lie within analytical error of each other and indicate that all magmas had similarly homogenous Hf isotope compositions.

The Fleet Pluton

Zircon ages yielded a weighted mean $^{206}Pb/^{238}U$ age of 394 ± 11 Ma (n = 14) for the entire pluton (Table 1). However, the outermost biotite granite zone gives a mean $^{206}Pb/^{238}U$ age of 410 ± 3 Ma (n = 4) that is distinct from that of the two inner muscovite-bearing zones, which lie within analytical error of each other and have a mean $^{206}Pb/^{238}U$ age of 387 ± 5 Ma (n = 11).

Zircons from the outer two zones of the Fleet pluton yielded mean oxygen isotope compositions of 6.8 ± 0.8 ‰ (2 SD; *n* = 15) and 7.1 ± 1.5 ‰ (2 SD; *n* = 15) respectively (Fig. 7). Zircons from the inner fine-grained biotite-muscovite granite yielded a mean value of 6.4 ± 1.7 ‰ (2 SD; *n* = 10). In the outer zone, 73% of analyses fall within analytical error of the mean, while 53% and 40% of analyses in the middle and inner-most zones respectively fall within analytical error of their mean population values.

Mean εHf_t values for each zone of the Fleet pluton lie largely within analytical error (0.8 εHf units) of each other (excluding two points with εHf <-10) but are lower than those of the Criffell pluton, with mean εHf_t values for each zone of: Zone 1 0.7 ± 0.6, Zone 2 = 0.1 ± 0.8 and Zone 3 = 1.2 ± 1.2 (1 SD group error).

The Shap Pluton

Zircon $^{206}Pb/^{238}U$ ages (Table 1) for the granitic samples lie within analytical error of each other and yielded a mean $^{206}Pb/^{238}U$ age of 416 ± 5 Ma (*n* = 11).

Mean zircon oxygen isotope compositions for both stage 1 and 2 granites of the Shap pluton lie within analytical precision of each other, with mean oxygen isotope compositions between 7.6‰ and 7.9‰ (Table 1; Fig. 7). 85% of analyses in the stage 1 population fall within analytical error of the population mean while 76% of analyses in the stage 2 population fall within analytical error of the population mean.

Mean Hf compositions lie within analytical error of each other, with group means of: Outer zone granite = -0.2 ± 0.4, Inner zone granite = -0.4 ± 0.6 (1 SD group error). These values are lower than those from the Criffell and Fleet plutons.

Dioritic enclaves

Diorite enclaves were studied from the Criffell and Shap plutons. Zircons from a diorite enclave in Zone 1 of the Criffell pluton have a mean $^{206}Pb/^{238}U$ age of 411 ± 3 Ma (n = 10), which is within analytical error of the mean age of its host granodiorite (408 ± 7 Ma (n = 9)) (Table 1). A second enclave from Zone 2 of the Criffell pluton yielded a mean $^{206}Pb/^{238}U$ age of 420 ± 4 Ma (n = 6), which is distinctly different in age from its granodiorite host (mean age of 409 ± 7 Ma (n = 9)). Dioritic enclaves from the Shap pluton have a mean $^{206}Pb/^{238}U$ age of 418 ± 4 Ma (n = 12) and are within analytical error of the granite hosts (Table 1).

Oxygen isotope compositions for zircons from the two Criffell enclaves have mean and 2 SD population values of 6.3 ± 0.5 ‰ (2SD; n = 15) and 6.2 ± 0.4 ‰ (2SD; n = 15) respectively and are generally more ^{18}O-rich relative to their host granodiorites (Fig. 9; Table 1). Mean oxygen isotope compositions for the Shap enclaves are indistinguishable from their host granites.

The mean εHf_t values of zircons extracted from all mafic enclaves lie within analytical error of their respective host granitoids.

In summary, U-Pb ages for all zones in the Criffell (410 ± 6 Ma) and Shap (416 ± 5 Ma) plutons lie largely within error of each other, By contrast, the outer zone of the Fleet pluton (410 ± 3 Ma) appears to be ~ 23 Myr older than the two inner zones (387 ± 5 Ma) and comparable in age to the Criffell and Shap plutons. Zircon $\delta^{18}O$ compositions generally increase as magmas become more silicic, with mean values ranging between ~ 5.8 ‰ to 7.9 ‰ within most plutons. There is a general increase in compositional heterogeneity between crystals in the Criffell and Fleet plutons as the magmas become more silicic. εHf compositions differ only between plutons and are largely homogenous within individual plutons. The most radiogenic compositions are found in the Criffell pluton (~ +2.4 to +4.4) and the least radiogenic in the Shap pluton (-0.2 to -0.4).

DISCUSSION

The new geochronological results presented here indicate that the TSS of granite plutons were emplaced during an early phase of post-collisional transtension (410-420 Ma) rather than during subsequent transpression as previously suggested (e.g. Halliday *et al*. 1980; Pidgeon and Aftallion, 1978; Wadge *et al*. 1978; Davidson *et al*. 2005; Brown *et al.* 2008). Within this framework, the increasing heterogeneity in zircon oxygen isotope compositions in more silicic zones of the TSS is discussed with reference to the involvement of mafic magmas in the formation of the peraluminous granites. Model ages are used to investigate the possibility that underthrust Avalonian basement was involved in the evolution of the plutons. These new findings are used to examine the interrelated magmatic and tectonic processes that have led to the distinguishing characteristics of the TSS relative to other post-Caledonian Devonian granites. These include their proximity to the Iapetus Suture at a time when subduction had ceased (see Stephenson, 1999 and references therein), despite their calc-alkaline compositions, the absence of inherited zircons despite strong chemical evidence for the partial melting and assimilation of sedimentary components (Pidgeon and Aftallion, 1978), and the similar ^{207}Pb isotope compositions of all the TSS plutons (Thirlwall, 1989).

New constraints on the emplacement history of the TSS

In contrast to the results of this study, most other published age data suggest that the TSS was emplaced between *c.* 400 and 390 Ma. We see no reason to doubt the analytical accuracy of our new ages (Supplementary Material 1), but it is clearly necessary to consider why these ages should differ significantly from those determined by other methods that were nonetheless often found to be in mutual agreement (see Brown *et al*. 2008 and references therein).

Many of the currently accepted ages for the TSS were determined using mineral-whole-rock Rb-Sr isochrons that were often in agreement with biotite and hornblende K-Ar ages (Halliday *et al*. 1980). The accuracy of both methods are however susceptible to the effects of element loss caused by alteration (particularly in plagioclase and biotite) and thermal re-setting. The Rb-Sr system in biotite and plagioclase is also subject to significantly lower closure temperatures (<350°C for Rb-Sr in biotite and plagioclase, Harland *et al*., 1990) than is required for U-Pb dating in zircon (*c*. >1000°C, Cherniak and Watson, 2001). Similar arguments can be used against K-Ar dating using biotite and hornblende. Cleavage in some TSS plutons such as Shap points to transient compressional events during or after the emplacement of some TSS plutons, while the Fleet pluton is said to document textural evidence for weak Aracdian deformation (Boulter & Soper 1973; Soper & Kneller, 1990; Lintern *et al*. 1992; Barnes *et al*. 1995; Phillips *et al*. 1995). It is possible that small, transient thermal perturbations associated with these events may have undermined the accuracy of Rb-Sr and K-Ar methods.

Zircon U-Pb ages reported by Pidgeon and Aftallion (1978) for all three plutons represent bulk analyses of various zircon size fractions. For individual plutons, emplacement ages were determined using upper intercepts between discordia and concordia that are frequently constrained by a very limited number (usually 3 or 4) of data points. Inspection of the intercept ages reveals that considerable age differences may be possible with the addition of further data points. Similar arguments can be made regarding the emplacement ages of the Shap and Fleet plutons.

A further possibility is that younger bulk zircon ages reflect the effects of later crystal overgrowths which may be evident in darker discordant rims in some CL images (Figs. 5a, e). These rims cannot be analysed by *in situ* methods due to beam-size limitations. However, the small volumes of crystal overgrowths present would require them to have significantly younger ages in order to account for the age discrepancy observed between bulk and *in situ* methods. The absence of zircon cores inherited from supracrustal source rocks has previously been interpreted to indicate that the current mineral assemblage crystallised following segregation and ascent of crystal-free magmas from a deep crustal hot zone (Miles *et al*. 2013). The *in situ* ages reported here therefore provide a *minimum* age for magma generation. These age estimates are consistent with magma generation in a tectonic regime apparently dominated by transtension (Brown *et al*. 2008) and are synchronous with regionally prolific lamprophyre dykes (Rock *et al*. 1986) and enhanced geothermal gradients in the slate belts of North Wales (Soper & Woodcock, 2003). However, the possibility of later emplacement, represented by thin zircon overgrowths, cannot be ruled out.

In addition, a mean zircon $^{206}Pb/^{238}U$ age of 387 ± 5 Ma for the two inner zones of the Fleet pluton is broadly consistent with the previous zircon U-Pb age estimates of Pidgeon & Aftalion (1978) and Halliday *et al*. (1980). However, a resolvable age difference is evident between the intrusion of these zones and that of the older and outer-most biotite zone which has a mean age of 410 ± 3 Ma. The inner two zones of the pluton were emplaced immediately following a proposed transpressional regime associated with a brief phase of Acadian compression (Fig. 10). The end-Acadian deformation has been difficult to constrain in Britain, but is thought to have ended by *c.* 390 Ma based on the K-Ar ages of illite in cleaved mudrocks (Soper and Woodcock 2003; Brown *et al*. 2008). Renewed extension following Acadian compression in the late Devonian is indicated by renewed deposition in the Strathmore Basin (Armstrong & Patterson, 1970) that may also be associated with the second phase of magmatism seen in the Fleet pluton. Deformation of cordierite in the thermal aureole of the Fleet pluton, together with biotite overgrowth of local cleavage, has previously been used to indicate coeval activity on the Moniaive Shear Zone and pluton emplacement (Lintern *et al*. 1992; Barnes *et al*. 1995; Phillips *et al*. 1995). New geochronological evidence for earlier emplacement of the outer zone of the Fleet pluton (410 Ma) presented here suggests that deformed minerals may be associated with the earlier intrusive phase while later biotite overgrowth of local cleavage may be associated with the second and later phase of emplacement (387 Ma). Reactivation of the Moniaive Shear Zone is therefore likely to have occurred between the two intrusive phases (410 to 387 Ma).

Isotopic constraints on the evolution of magma compositions

Oxygen Isotope compositions of zircons

In addition to providing a new timeframe for the emplacement of the TSS, zircons have yielded oxygen isotope compositions that enable a number of magmatic sources to be identified and distinguished. Under closed system conditions where magma differentiation is controlled by crystallisation alone, all minerals should remain in isotopic equilibrium and melt-zircon fractionation factors (Δ(melt-Zrc)) should increase with increasing SiO_2 (Valley *et al*. 1994). It follows that compositional variability greater than analytical error (~ 0.6 ‰) can only result from the addition of isotopically distinct materials.

The total range in zircon $\delta^{18}O$ is up to ~ 4 ‰ in the Criffell pluton, ~ 3.5 ‰ in the Fleet pluton and ~ 1.3‰ in Shap (Figs. 7 and 8). The range of values observed in the former two plutons requires the assimilation (or mixing) of material from compositionally distinct sources, consistent with the variations in $^{87}Sr/^{86}Sr$ and εNd reported by Halliday (1984) and Halliday *et al*. (1980) in the whole-rock suites. Zircon populations in individual samples from the outer zones of the Criffell and Fleet plutons have unimodal $\delta^{18}O$ distributions that lie mainly within analytical error of their means (2 SD in the populations of between 0.6 and 0.8 ‰). However, with increasing whole-rock SiO_2, mean $\delta^{18}O(Zrc)$ compositions in magmatic zircons generally increase in tandem with $\delta^{18}O$ heterogeneity within sample populations (Fig. 7). These observations imply that there was a range in magma compositions at the time of zircon crystallisation, and that in some cases zircons from different magma batches may have been preserved within the same whole-rock sample. The existence of primary magmatic zircons with more primitive isotope compositions than is consistent with their host whole-rock compositions has been noted from other peraluminous granites (e.g. Appleby *et al*. 2010; Kemp *et al*. 2006a; 2009). The cryptic evidence for the involvement of mafic magmas in the genesis of peraluminous granites signals a potentially important role for such granites in the formation of stable new continental crust (see Hawkesworth *et al*. 2010).

Mafic enclaves

The Nd isotope compositions of mafic dioritic enclaves from the Criffell pluton were found to be ~ 1 to 2 εNd units more radiogenic (-0.7 to +1.6) than their host granodiorites (-2.0 to +0.6), a difference that indicates that they do not originate from restite separation or cumulate formation from their host rocks (Holden, *et al*. 1987; Holden *et al.* 1991). New U-Pb ages obtained using zircons separated from one such enclave from Zone 2 reveal a mean age of 420 ± 4 Ma. This age is significantly older than that of another mineralogically similar enclave in Zone 1 (411 ± 4 Ma), and its host granodiorite (409 ± 7 Ma) (Table 1). Zircon U-Pb ages therefore support other, independent isotopic evidence (Holden, *et al*. 1987; Holden *et al.* 1991) for distinct magmatic histories for both the granodiorites and their enclaves. The oxygen isotope compositions of zircons from both enclaves in the Criffell pluton show unimodal distributions, with all grains falling within analytical error of their means (Fig. 9). Mean zircon $\delta^{18}O$ for both enclaves is ~ 0.5 ‰ higher than the mean $\delta^{18}O$ of their host granodiorites and both the enclaves studied have more limited $\delta^{18}O$ distributions (± 0.4 - 0.5 ‰ 2SD), providing further evidence of discrete origins. The mineral assemblage of the mafic enclaves has been successfully used to model the evolution of whole-rock compositions assuming fractional crystallisation and assimilation of Avalonian (Skiddaw-like) sediments (Stephens *et al*. 1985; Miles *et al*. 2013). The older ages reported from zircons separated from some of the enclaves, together with different whole-rock isotope compositions, may support the interpretation that the mafic enclaves in the Criffell pluton represent entrained, cognate assemblages from a crustal hot zone (Annen *et al*. 2002; 2006; Miles *et al.* 2013). U-Pb ages together with zircon oxygen isotope compositions from mafic enclaves in the Shap pluton lie largely within error of their hosts (Fig. 9), and their formation cannot easily be distinguished from that of their host magmas.

Isotope evidence for crustal reworking

The whole-rock compositions of late- and post-Caledonian Devonian granites throughout Scotland have undoubtedly provided valuable information about the large-scale divisions of lower crustal domains (Frost & O'Nions, 1985; Halliday *et al*. 1980; Hamilton *et al*. 1980; Harmon & Halliday, 1980; Pidgeon & Aftalion, 1978). However, the characteristics of individual sources remain ambiguous and it is unclear whether the TSS is the product of mantle-derived magmas contaminated by crustal components, reflecting net additions to the continental crust, or resulted entirely from crustal reworking (Clayburn *et al*. 1983; Halliday 1984; Halliday *et al*. 1980; Harmon & Halliday 1980; Frost & O'Nions 1985). The O-Hf isotopic compositions of magmatic zircons have recently provided a further means of distinguishing and characterising different source contributions, together with the relative proportions of crustal growth and reworking (e.g. Appleby *et al*. 2010; Hawkesworth & Kemp, 2006; Kemp *et al*. 2007; Marschall *et al*. 2010).

Between ~ 50% and 62% of zircon crystals from the more mafic outer two zones of Criffell have oxygen isotope compositions that fall within the accepted range of mantle-like compositions (5.3 ± 0.6 ‰; Valley *et al*. 1998). Such compositions may either reflect magmas derived directly from the mantle or from juvenile lower crust, because of a lack of oxygen isotope fractionation at lower crustal temperatures. If derived from the mantle, their compositions may therefore represent net additions to the crust. By contrast, more evolved zones of Criffell contain only ~ 5% mantle-like zircons, compared to up to 30% in the inner and most evolved zone of the Fleet pluton (Fig. 7). In these zones, the majority of zircons therefore have $\delta^{18}O$ compositions that exceed those in equilibrium with mantle or juvenile lower crust and instead reflect reworking of ^{18}O-rich upper crustal material. No zircons from the Shap pluton exhibit mantle-like compositions (Fig. 8).

In contrast to oxygen isotopes, the initial εHf_t values of all zircons from all three plutons are lower than those of contemporaneous depleted mantle (~ +16 ± 3; Vervoort *et al.* 1999), where the variability of ± 3 εHf units is estimated from present-day variations in MORB (Griffin *et al*. 2000; Fig. 11). However, enriched mantle compositions may be similar to zircon compositions in the Criffell pluton. Characterising Devonian mantle compositions in the Iapetus Suture region is therefore crucial for estimating relative mantle and crustal contributions in the TSS.

Enriched mantle compositions have been identified from the εNd compositions of mantle-derived mafic magmas of upper Silurian to Lower Devonian (~ 416 Ma) age across Scotland (Thirlwall, 1982). In detail, enriched mantle components with initial εNd values between +1.1 and -3.6 (estimated εHf = +3.6 to -2.9) have been found *north* of the Highland Boundary Fault. However, upper Silurian to Lower Devonian (~ 416 Ma) age calc-alkaline lavas *south* of the Highland Boundary fault, close to the TSS, have initial εNd values up to +6.4 (estimated εHf_t values of +11.4) that are more characteristic of depleted mantle. Some offset to more radiogenic Sr relative to the Sr-Nd mantle array is thought to reflect earlier subduction-related modification of a predominantly depleted mantle (Thirlwall, 1982). It is therefore more likely that any mantle contributions to the TSS were sourced within depleted and not enriched mantle.

Variability in zircon εHf_t compositions is very limited among zircons from individual plutons, but they vary between plutons by ~ 5 εHf units. The most positive and mantle-like zircon εHf_t compositions are found in the Criffell pluton (+3.4 ± 0.5), while the most negative and crust-like values are found in the Shap pluton (-0.4 ± 0.5) with intermediate values in the Fleet pluton (+0.6 ± 0.9). The εHf_t data therefore suggest that all zircon compositions formed from either non-mantle sources or by the hybridisation of mantle and crustal components. This evidence illustrates the importance of integrated O-Hf isotope studies to distinguish mantle and lower-crustal source regions, both of which frequently have indistinguishable $\delta^{18}O$ compositions. This compositional similarity reflects limited isotope fractionation between coexisting minerals, melts and fluids at mantle and lower crustal temperatures (Bindeman, 2008).

Granite sources in the Iapetus Suture Zone

The identity of crustal sources in each of the TSS plutons is difficult to constrain due mainly to the absence of basement exposure. Zircon O-Hf arrays reveal two apparent trends (Fig. 11), one defined at an inter-pluton scale, extending from radiogenic (Criffell) to less radiogenic (Shap) εHf_t compositions, and the second at an intra-pluton scale, ranging from low to high ^{18}O compositions with little variation in εHf_t.

Inter-pluton $\delta^{18}O$-εHf_t trend

Differences in zircon εHf_t between different plutons may indicate discrete sources for each of the three plutons, or that each lies at a different position along a single mixing curve between primitive and evolved source regions. A source or sources common to all three plutons is favoured by the persistent occurrence of high $^{207}Pb/^{204}Pb$ compositions in all plutons (Thirlwall, 1989) (Fig. 6). Whole-rock Pb isotope compositions also preclude involvement of Southern Uplands sediments in the genesis of the TSS (Thirlwall, 1989; Miles *et al*. 2013) and mean that all potential sources reside at depths that exceed the thickness of the Southern Uplands sediment pile, which Stephenson (1999) suggests extends to depths equivalent to the Iapetus Suture itself. All potential sources must therefore lie within or below the Avalonian terrane that underlies the suture. Elevated Pb isotope compositions have previously been linked to sedimentary rocks with a similar composition to the Skiddaw Group found in the English Lake District (Thirlwall *et al*. 1989; Miles *et al*. 2013). However, Pb isotope compositions in the Fleet pluton extend to even more radiogenic compositions than the Skiddaw Group (Fig. 6) and suggest that an underlying crustal component within the Avalonian terrane may also be involved.

Model ages provide a potential means of identifying and characterising the magmatic sources involved in the formation of the TSS. Dhuime *et al*. (2011) point out that juvenile crust generated in modern arcs does not resemble the Hf isotope composition of depleted mantle and as such, model ages should be calculated using the 'new crust' reference line and not depleted mantle. Only zircons with mantle-like oxygen isotope compositions can be considered to provide Hf model ages that reliably date crustal extraction from the mantle (Dhuime *et al*. 2012). Those with more ^{18}O-enriched isotope compositions reflect crustal reworking and provide only hybrid model ages with little geological significance. However, zircons from the three TSS suite plutons studied show limited variation in Hf despite larger intra-pluton variations in ^{18}O. In the case of the three plutons studied and when calculating Hf model ages, there is therefore no need to limit the selection of crystals to mantle-like zircons. Model ages using zircons from the Criffell pluton, calculated using the 'new crust' reference curve, suggest ages of ~ 0.9 to 1.0 Ga (Fig. 12).

Due to a lack of exposure, model ages for the Avalonian basement have relied on Sm-Nd analyses from Neoproterozoic to Early Silurian igneous rocks thought to be derived almost exclusively from remelting of Avalonian basement (e.g. Ayuso, 1986; Murphy *et al*. 2000; Nance *et al*. 2008; Nance and Murphy, 1996). Confirmation of basement isotopic compositions has come from close similarities in the calculated Nd model ages of arc-related igneous rocks formed across a range of different periods throughout the Avalonian terrane. Most studies suggest that the Avalonian basement was generated in a series of ocean island arcs between 1.2 and 1.0 Ga (Murphy *et al*. 2000). In the UK, the Malvern Plutonic Complex (~ 677 Ma) is thought to provide one of the only opportunities to examine the Avalonian basement, yielding model ages of between 1.2 and 1.0 Ga (Thorogood, 1990), similar to estimates from other regions of Avalonia (Murphy *et al*. 2000). However, these model ages assume that new crust resembles the Nd compositions of depleted mantle. In order to enable more reliable comparisons between the Hf model ages calculated in this study and published data on Avalonian basement, a new crustal reference line for Nd isotopes has been estimated. This uses the εHf_t composition of 'new crust' ($\varepsilon Hf = +13.2$, Dhuime *et al*. 2011) together with a Nd-Hf relationship of $\varepsilon Hf = 1.40\varepsilon Nd + 2.1$ (Vervoort *et al*. 1999). Model ages for Avalonian basement calculated using a 'new crust' curve for Nd range between ~ 1.0 and 1.1 Ga.

The age of the Laurentian basement has primarily been determined using detrital zircons from the Dalradian Supergroup, where age peaks at 2.7, 1.8 and 1.1 Ga reflect major episodes of Laurentian crustal growth (Hoffman, 1989; Cawood *et al*. 2003; Waldron *et al*. 2008). Although some model age estimates for the TSS may match the 1.1 Ga peak, there is no evidence of other characteristic age peaks in the TSS indicative of Laurentian basement. Importantly, this conclusion is not changed if the depleted mantle reference line is used for calculating TSS model ages.

The similarities observed between the model ages of proposed Avalonian basement and those of the TSS of plutons suggest that a significant proportion of Avalonian re-working was involved in the formation of this granite suite. The slightly younger model ages estimated using zircons from the Criffell pluton relative to Avalonian basement model ages may reflect small contributions from depleted mantle or an additional juvenile source. In general, Hf isotope compositions support independent seismic evidence for the underthrusting of Avalonian crust beneath the

Laurentian margin (Beamish & Smythe, 1986; Freeman *et al*. 1988; Hall *et al.* 1984; Klemperer & Matthews, 1987; Klemperer *et al*. 1991) and similarities in the Pb isotope compositions of TSS plutons and Avalonian sediments (Fig. 6) (Thirlwall, 1989).

Intra-pluton $\delta^{18}O$-εHf_t trends

Intra-pluton trends are characterised by variations in the degree of ^{18}O enrichment (Fig. 11) and are highly indicative of supracrustal contributions. Pb isotope compositions in the whole-rock suite (Thirlwall, 1989) indicate that the sediments are likely to be similar in composition to the Skiddaw Group (Fig. 6). Average $\delta^{18}O$ (12.7 ± 1.6 ‰ 1SD) and εHf (-6.5 ± 2.4 1SD) compositions for the Skiddaw Group sediments have been estimated using published data from Thomas *et al*. (1985) and Stone & Evans (1997), with oxygen isotope compositions recalculated to give equilibrium zircon oxygen isotope compositions. O-Hf trends are essentially vertical for each of the plutons (Fig. 11), precluding linear mixing trends between the most primitive components in each pluton and Skiddaw Group sediments. Any mixing between primitive components and Skiddaw Group sediments must therefore follow concave down trajectories, examples of which have been modelled in Figure 11. These models suggest sediment contributions of up to *c.* 50% in the most peraluminous zones of the Criffell pluton. Equivalent calculations for the Fleet pluton also indicate sedimentary contribution of up to ~50%.

Together, the isotopic compositions of whole-rock and magmatic zircon provide a means of identifying and characterising some of the sources involved in the formation of the TSS. The NW-SE cross-section along the UK Geotraverse North line shown in Figure 13a is based on seismic interpretations (Freeman *et al*. 1988; Hall *et* *al.* 1984; Klemperer & Matthews, 1987; Klemperer *et al*. 1991; Soper *et al*. 1992; Brown *et al.* 2008) and illustrates the geometrical relationships between Laurentian and Avalonian lithospheric components. The underthrusting of Avalonian lithosphere beneath the Laurentian margin is suggested by both seismic evidence and the occurrence of Pb isotope compositions in the TSS that more closely resemble those of Avalonian components (Fig. 13b) (Thirlwall, 1989). The Fleet pluton shows evidence for a further, more ^{207}Pb-rich component beneath the suture that may represent unexposed Avalonian basement. Hf and O isotope compositions alone (Fig. 13b-c) evidently do not distinguish Avalonian and Laurentian crustal components, but are at least consistent with the involvement of Avalonian crust in the genesis of the TSS granitic magmas. However, Hf model ages are consistent with the involvement of Avalonian basement (Fig. 12). Oxygen isotopes together with the more mantle-like Hf compositions of some zircons from the Criffell pluton indicate the possible involvement of depleted mantle in the formation of the TSS which may also have served as a heat source for subsequent crustal melting. Such mantle contributions are consistent with the synchronous intrusion of lamprophyre dykes (Fig. 13a). Many uncertainties remain regarding the detailed nature and identity of the source rocks beneath the Iapetus Suture. However, seismic and isotopic data together suggest that crustal hot zones, in which the magma compositions were predominantly determined were located beneath the Laurentia-Avalonia suture at depths of > 20 km beneath the Fleet pluton and > 11 km beneath the Criffell pluton (Fig. 13).

Tectonic controls on pluton formation and emplacement

The calc-alkaline compositions of the TSS together with their proximity to the former Iapetus subduction zone have presented a significant challenge to understanding the tectonic and magmatic evolution of the region. Despite evidence for periods of transtension following closure of the Iapetus Ocean at ~ 420 Ma, previous age estimates suggest that the TSS plutons were emplaced during periods of transpression at ~ 400 to 390 Ma (see Brown *et al*. 2008 and references therein). Reconciling the formation of granite plutons with tectonic evidence of transpression has led to the suggestion of 'incipient delamination' discussed previously and linked to changes in the distribution of vertical stresses following lithospheric shortening (O'Reilly *et al*. 2012). The new U-Pb ages reported here show that all three TSS plutons studied were emplaced during phases of transtension before ~ 400 Ma and after ~ 390 Ma (Fig. 10). It is therefore unnecessary to appeal to mechanisms such as 'incipient delamination' and likely that the simultaneous intrusion of mafic lamprophyre dykes (Rock *et al*. 1986) and the TSS granite plutons resulted primarily from passive melting and heat transfer into the crust during lithospheric transtension (see Brown *et al*. 2008).

Transtension is a characteristic tectonic feature of oblique continental convergence that is increasingly being recognised as an important factor in the formation and preservation of granitic plutons (e.g. Tikoff & Teyssier, 1992; Grocott *et al*. 1994; Teyssier *et al*. 1995; Dewey, 2002; Hanson & Glazner, 1995; Paterson & Fowler, 1993; Weinberg *et al*. 2004; Kemp *et al*. 2009; Kirsch *et al*. 2012; Hawkesworth *et al*. 2010). Granites in the Lachlan Fold Belt (SE Australia) have been shown to represent changing net additions to the local continental crust that reflects the interplay of transtension and transpression, albeit during active subduction (Kemp *et al*. 2009). This study has shown that metaluminous granites, similar in compositions to the metaluminous components of the TSS represent ~ 70% new crustal growth, confirming the importance of extensional tectonic regimes in creating new crustal material. Furthermore, the zircon O-Hf isotope compositions of the peraluminous granites of the Lachlan Fold Belt, generated during phases of crustal thickening, have been shown to contain up to ~30% mantle material. These results mirror the discovery of cryptic signatures of mafic magma involvement in the peraluminous plutons of this study and in other recent micro-analytical studies that suggest that peraluminous granites may also represent net additions to the continental crust (Appleby *et al*. 2010).

The absence of inherited zircons in the TSS has also been used to distinguish them from other Devonian granites throughout Scotland (Pidgeon & Aftalion, 1978). However, with strong evidence for the involvement of supracrustal components in the formation of the TSS together with continued zircon saturation throughout magma evolution (Miles *et al*. 2013), the absence of inherited zircon is unlikely to reflect source characteristics or dissolution in zircon-undersaturated melts. Instead, it is more likely to reflect distinct magmatic processes in the TSS relative to other Devonian granites. The absence of inherited zircons together with the calc-alkaline composition of the TSS are considered to result from the elevated water contents of the magmas, while the former characteristic is thought to reflect crystal resorption during hydrous magma ascent under super-liquidus conditions (Miles *et al*. 2013). Elevated water contents in the TSS relative to Devonian plutons further north in Scotland is consistent with their proximity to the former Iapetus Suture, where prolonged dehydration of subducted Iapetus oceanic crust is likely to have occurred, analogous to the early Basin and Range suites in the western United States (Humphreys *et al*. 2003). Significant hydration of the underlying mantle lithosphere is also evident from the regionally prolific occurrence of lamprophyre dykes in and around the Iapetus Suture (Rock *et al*. 1986).

There is therefore good evidence that the unusual characteristics of the TSS plutons, including lack of inherited zircons and their proximity to the suture zone, reflect the unique tectonic and crustal setting in which their genesis and emplacement took place.

CONCLUSIONS

New zircon U-Pb ages confirm that the Criffell and Shap plutons were emplaced earlier than previously thought, with mean ages of 410 ± 6 Ma and 416 ± 5 Ma for the Criffell and Shap plutons respectively. An age of 410 ± 3 Ma for the outer zone of the Fleet pluton is also considerably older than previous estimates; however, the two inner zones reveal a mean age of 387 ± 5 Ma and demonstrate a protracted history of pluton growth. These new ages confirm that pluton emplacement occurred during an inferred stage of transtension, coinciding with the regional intrusion of a lamprophyre dyke swarm. The emplacement of the inner zones of the Fleet pluton may coincide with post-Acadian extension.

Zircon oxygen isotope compositions in different zones of the Criffell, Fleet and Shap plutons show intra-zone variability at the pluton scale consistent with open-system differentiation. At an intra-sample scale, zircons in more primitive granodiorites are isotopically homogeneous, while greater isotopic variation is evident amongst zircon crystals in more silicic zones, reflecting the preservation of compositionally diverse magmas prior to crystallisation. The occurrence of more primitive zircon oxygen isotope compositions in the more silicic zones also reflects the involvement of more mafic magmas in the formation of large peraluminous plutons such as Fleet.

Mafic enclaves in the Criffell pluton contain zircons with different oxygen isotope compositions and in one example mean U-Pb ages are ~9 Myr older than their hosts. They are considered to represent entrained cognate material in segregated magma batches, derived potentially from regions of magma generation and differentiation in lower crustal hot zones.

Zircon εHf_t values are distinct and show little variation in each of the Criffell, Fleet and Shap plutons. Zircon εHf_t compositions in all plutons reveal model ages consistent with the involvement of Avalonian basement in magma genesis. Previous Pb isotope studies (Thirlwall, 1989) have confirmed the absence of local Southern Uplands sediments in the origin and evolution of the TSS plutons and instead point to the involvement of sedimentary components found in the underthrust Avalonian terrane. Hf model ages in all TSS plutons, calculated using the most mantle-like zircons, are similar to estimated model ages for Avalonian basement. Further mixing with up to 50% of a sedimentary component similar to the Skiddaw Group which overlies the Avalonian terrane is capable of reproducing intra-pluton trends of ^{18}O enrichment in zircons from the Criffell and Fleet plutons. The integration of zircon isotopic data with geological and geophysical data on crustal structure and lithologies across the Iapetus Suture Zone has provided a much deeper and more detailed insight into the genesis and evolution of the TSS granites.

Evidence for high water contents in these granites linked to the adiabatic ascent and resorption of entrained crystals (Miles *et al*. 2013) reflects the importance of hydrated lithosphere in magma genesis. This may in turn have resulted from earlier dehydration of the subducting Iapetus oceanic crust and is consistent with the extensive occurrence of lamprophyric dykes and calc-alkaline granitoids of the same age around the suture zone. Many of the unusual chemical and physical characteristics that distinguish these calc-alkaline granites from other late and post-Caledonian granites can therefore be linked to their emplacement and formation during crustal transtension within the Iapetus suture zone.

ACKNOWLEDGMENTS

We thank John Craven for technical support with ion probe analyses and the Bristol laser group for Hf analytical time. Nicola Cayzer is thanked for assistance with SEM imaging. Ed Stephens and Nigel Woodcock have provided valuable knowledge of granite genesis and regional geology respectively. Angus Calder and Donald Herd assisted with heavy mineral separation at the University of St Andrews. Rita Economos, Stephen Daly and an anonymous reviewer are thanks for insightful reviews that have greatly improved the manuscript. John Gamble is thanked for editorial handling.

FUNDING

This work was supported by a NERC CASE studentship NE/G524128/1

REFERENCES

Annen, C., Blundy, J.D. & Sparks, R.S.J. (2006). The genesis of intermediate and silicic magmas in deep crustal hot zones. *Journal of Petrology* **47**, 505-539.

Annen, C. & Sparks, R.S.J. (2002). Effects of repetitive emplacement of basaltic intrusions on thermal evolution and melt generation in the crust. *Earth and Planetary Science Letters* **203**, 937-955.

Appleby, S.K., Gillespie, M.R., Graham, C.M., Hinton, R.W., Oliver, G.J.H., Kelly, N.M. & EIMF (2010). Do Peraluminous granites commonly sample infracrustal sources? New results from an integrated O, U-Pb and Hf isotope study of zircon. *Contributions to Mineralogy and Petrology* **160**, 115-132.

Appleby, S.K., Graham, C.M., Gillespie, M.R., Hinton, R.W., Oliver, G.J.H. & EIMF. (2008). A cryptic record of magma mixing in diorites revealed by high-precision SIMS oxygen isotope analysis of zircons. *Earth and Planetary Science Letters* **269**, 105-117.

Armstrong, M. & Paterson, I.B. (1970). The Lower Old Red Sandstone of the Strathmore region. *Report of the Institute of Geological Sciences* 70/12.

Atherton, M.P. & Ghani, A.A. (2002) Slab breakoff: a model for Caledonian, Late Granite syn-collisional magmatism in the orthotectonic (metamorphic) zone of Sctland and Donegal, Ireland. *Lithos* **62**, 65-85.

Ayuso, R.A. (1986). Lead-isotopic evidence for distinct sources of granite and for distinct basements in the northern Appalachians, Maine. *Geology* **14**, 322-325.

Barnes, R.P., Lintern, B.C. & Stone, P. (1989). Timing and regional implications of deformation in the Southern Uplands of Scotland. *Journal of the Geological Society* **146**, 905-908.

Barnes, R.P., Phillips, E.R. & Boland, M.P. (1995). The Orlock Bridge Fault in the Southern Uplands of Southwestern Scotland - A terrane boundary. *Geological Magazine* **132**, 523-529.

Beamish, D. & Smythe, D.K. (1986). Geophysical images of the deep crust: the Iapetus suture. *Journal of the Geological Society* **143**, 489-497.

Bindeman, I. (2008) *Oxygen Isotopes in Mantle and Crustal Magmas as Revealed by Single Crystal Analysis*. In: Putirka K..D. & Tepley F.J. (ed) *Minerals, Inclusions and Volcanic Processes*, vol 69. pp 445-478.

Bluck, B. (1983). Role of the Midland Valley of Scotland in the Caledonian Orogeny. *Transactions of the Royal Society of Edinburgh-Earth Sciences* **74**, 119-136.

Boulter, C.A. & Soper, N.J. (1973). Structural relationships of the Shap granite. *Proceedings of the Yorkshire Geological Society* **39**, 365-369.

Bouvier, A., Vervoort, J.D. & Patchett, P.J. (2008). The Lu-Hf and Sm-Nd isotopic composition of CHUR: Constraints from unequilibrated chondrites and implications for the bulk composition of terrestrial planets. *Earth and Planetary Science Letters* **273**, 48-57.

Bradley, D.C. (2011). Secular trends in the geologic record and the supercontinent cycle. *Earth-Science Reviews* **108**, 16-33.

Brown, P.E., Ryan, P.D., Soper, N.J. & Woodcock, N.H. (2008). The Newer Granite problem revisited: a transtensional origin for the Early Devonian Trans-Suture Suite. *Geological Magazine* **145**, 235-256.

Campbell, I.H. & Taylor, S.R. (1983). No water, no granites - no oceans, no continents *Geophysical Research Letters* **10**, 1061-1064.

Canning, J.C., Henney, P.J., Morrison, M.A. & Gaskarth, J.W., (1996) Geochemistry of late Caledonian minettes from northern Britain: implications for the Caledonian sub-continental lithospheric mantle. *Mineralogical Magazine*, **60**, 221-236.

Cavosie, A.J., Valley, J.W. & Wilde, S.A. (2005). Magmatic delta O-18 in 4400-3900 Ma detrital zircons: A record of the alteration and recycling of crust in the Early Archean. *Earth and Planetary Science Letters* **235**, 663-681.

Cawood, P.A., Nemchin, A.A., Smith, M., & Loewy, S. (2003). Source of the Dalradian Supergroup constrained by U-Pb dating of detrital zircon and implications for the East Laurentian margin. *Journal of the Geological Society,* London **160**, 231–246.

Chappell, B.W. & White, A.J.R. (1974). Two contrasting granite types. *Pacific Geology* **8**, 173-174.

Cherniak, D.J., & Watson, E.B., 2001, Pb diffusion in zircon: *Chemical Geology*. **172**, 5-24.

Clayburn, J.A.P., Harmon, R.S., Pankhurst, R.J. & Brown, J.F. (1983). Sr, O, and Pb isotope evidecne for origin and evolution of Etive igneous complex, Scotland. *Nature* **303**, 492-497.

Cooper, M.R., Crowley, Q.G., Hollis, S.P., Noble, S.R. & Henney, P.J. (2013). A U-Pb age for the Late Caledonian Sperrin Mountains minor intrusions suite in the north of Ireland: timing of slab break-off in the Grampian terrane and the significance of deep-seated, crustal linements. *Journal of the Geological Society*, London **170**, 603-614.

Cox, R.A., Dempster, T.J., Bell, B.R. & Rogers, G. (1996). Crystallization of the Shap granite: Evidence from zoned K-feldspar megacrysts. *Journal of the Geological Society* **153**, 625-635.

Davidson, J., Charlier, B. & Hora, J.M. (2005). Mineral isochrons and isotopic fingerprinting: Pitfalls and promises. *Geology* **33**, 29-32.

DePaolo, D.J. (1981). Trace element and isotopic effects of combined wallrock assimilation and fractional crystallization. *Earth and Planetary Science Letters* **53**, 189–202.

Dewey, J.F. (2002). Transtension in arcs and orogens. *International Geology Review* **44**, 402-439.

Dewey, J.F. & Strachan, R.A. (2003). Changing Silurian-Devonian relative plate motion in the Caledonides: sinistral transpression to sinistral transtension. *Journal of the Geological Society* **160**, 219-229.

Dhuime, B., Hawkesworth, C. & Cawood, P. (2011). When Continents Formed. *Science* **331**, 154-155.

Dhuime, B., Hawkesworth, C.J., Cawood, P.A. & Storey, C.D. (2012). A Change in the Geodynamics of Continental Growth 3 Billion Years Ago. *Science* **335**, 1334-1336

Freeman, B., Klemperer, S.L. & Hobbs, R.W. (1988). The deep structure of Northern England and the Iapetus Sure Zone from BIRPS deep seismic reflection profiles *Journal of the Geological Society* **145**, 727-164.

Frost, C.D. & O'Nions, R.K. (1985). Caledonian Magma Genesis and Crustal Recycling. *Journal of Petrology* 26, 515-544.

Granthem, D.R. (1928). The petrology of the Shap granite. *Proceedings of the Geologists' Association* **39**, 299-331.

Gray, C.M. (1984). An isotopic mixing model for the origin of granitic-rocks in southeastern Australia. *Earth and Planetary Science Letters* **70**, 47-60.

Griffin, W.L., Pearson, N.J., Belousova, E., Jackson, S.E., van Achterbergh, E., O'Reilly, S.Y. & Shee, S.R. (2000). The Hf isotope composition of cratonic mantle: LAM-MC-ICPMS analysis of zircon megacrysts in kimberlites. *Geochimica Et Cosmochimica Acta* **64**, 133-147.

Griffin, W.L., Wang, X., Jackson, S.E., Pearson, N.J., O'Reilly, S.Y., Xu, X. & Zhou, X. (2002) Zircon chemistry and magma mixing, SE China: In-situ analysis of Hf isotopes, Tonglu and Pingtan igneous complexes. *Lithos* **61**, 237-269.

Grocott, J., Brown, M., Dallmeyer, R.D., Taylor, G.K. & Treloar, P.J. (1994). Mechanisms of continental growth in extensional arcs: An example from the Andean plate-boundary zone. *Geology* **22**, 391-394.

Hall, J., Brewer, J.A., Matthews, D.H. & Warner, M.R. (1984). Crustal structure across the Caledonides from the 'WINCH seismic reflection profile: Influences on the evolution of the Midland Valley of Scotland. *Transactions of the Royal Society of Edinburgh-Earth Sciences* **75**, 97-109.

Halliday, A.N. (1984). Coupled Sm-Nd and U-Pb Systematics in Late Caledonian Granites and the Basement under Northern Britain. *Nature* **307**, 229-233.

Halliday, A.N., Stephens, W.E. & Harmon, R.S. (1980). Rb-Sr and O Isotopic Relationships in 3 Zoned Caledonian Granitic Plutons, Southern Uplands, Scotland - Evidence for Varied Sources and Hybridization of Magmas. *Journal of the Geological Society* **137**, 329-348.

Hamilton, P.J., O'Nions, R.K. & Pankhurst, R.J. (1980). Isotopic Evidence for the Provenance of Some Caledonian Granites. *Nature* **287,** 279-284.

Hanson, R.B. & Glazner, A.F. (1995). Thermal requirements for extensional emplacement of granitoids. *Geology* **23**, :213-216

Harland, W.B., Armstrong, R.L., Cox, A.V., Craig, L.E., Smith, A.G. & Smith, D.G., 1989. A Geological Time Scale. Cambridge University Press, Cambridge, p. 263.

Harmon, R.S. & Halliday, A.N. (1980). Oxygen and strontium isotope relationships in the British Caledonian granites. *Nature* **283**, 21-25.

Harmon, R.S., Halliday, A.N., Clayburn, J.A.P. & Stephens, W.E. (1984). Chemical and isotopic systematics of the Caledonian intrusions of Scotland and Northern England - A guide to magma source regions and magma crust interaction. Philosophical Transactions of the Royal Society of London Series a-Mathematical Physical and Engineering Sciences **310**, 709-742.

Hawkesworth, C.J., Dhuime, B., Pietranik, A.B., Cawood, P.A., Kemp, A.I.S. & Storey, C.D. (2010). The generation and evolution of the continental crust. *Journal of the Geological Society* **167**, 229-248.

Hawkesworth, C.J. & Kemp, A.I.S. (2006). Using hafnium and oxygen isotopes in zircons to unravel the record of crustal evolution. *Chemical Geology* **226**, 144-162.

Highton, A. (1999). *Late Silurian and Devonian granitic intrusions of Scotland*. In: Stephenson, D., Bevins, R.E., Millward, D., Highton, A.J., Parsons, I., Stone, P., Wadsworth, W.J. (ed) *Caledonian Igneous Rocks of Britain*, vol Geological Conservation Review Series: Joint Nature Conservation Committee. pp 397-404.

Hoffman, P.F. (1989). Precambrian geology and tectonic history of North America, In Bally, A.W., and Palmer, A.R., (ed) *The Geology of North America: An Overview: Boulder, Colorado*, Geological Society of America, Geology of North America vol. A, pp 447-512.

Holden, P., Halliday, A.N. & Stephens, W.E. (1987). Neodymium and Strontium Isotope Content of Microdiorite Enclaves Points to Mantle Input to Granitoid Production. *Nature* **330**, 53-56.

Holden, P., Halliday, A.N., Stephens, W.E. & Henney, P.J. (1991), Chemical and isotopic evidence for major mass transfer between mafic enclaves and felsic magma. *Chemical Geology* **92**, 135-152.

Humphreys, E., Hessler, E., Dueker, K., Farmer, C.L., Erslev, E. & Atwater, T. (2003) How Laramide-age hydration of North American lithosphere by the Farallon slab controlled subsequent activity in the western United States. *International Geology Review* **45**, 575-595.

Hutton, D.H.W. & Reavy, R.J. (1992). Strike-slip tectonics and granite petrogenesis *Tectonics* **11**, 960-967.

Ireland, T. & Williams, I.S., (2003). *Considerations in zircon geochronology by SIMS*. In: Hanchar J.M. & Hoskin P.W.O. (ed) *Zircon*, vol 53. pp 215-241.

Jahn, B.M., Wu, F.Y. & Chen, B. (2000). Granitoids of the Central Asian Orogenic Belt and continental growth in the Phanerozoic. *Transactions of the Royal Society of Edinburgh-Earth Sciences* **91**, 181-193.

Keay, S., Collins, W.J. & McCulloch, M.T. (1997) A three-component Sr-Nd isotopic mixing model for granitoid genesis, Lachlan fold belt, eastern Australia. *Geology* **25**, 307-310.

Kelly, N.M., Hinton, R.W., Harley, S.L. & Appleby, S.K. (2008). New SIMS U-Pb zircon ages from the Langavat Belt, South Harris, NW Scotland: implications for the Lewisian terrane model. *Journal of the Geological Society* **165**, 967-981.

Kemp, A.E.S. (1987). Tectonic Development of the Southern Belt of the Southern Uplands Accretionary Complex. *Journal of the Geological Society* **144**, 827-838.

Kemp, A.I.S., Hawkesworth, C.J., Foster, G.L., Paterson, B.A., Woodhead, J.D., Hergt, J.M., Gray, C.M. & Whitehouse, M.J. (2007). Magmatic and crustal differentiation history of granitic rocks from Hf-O isotopes in zircon. *Science* **315**, 980-983.

Kemp, A.I.S., Hawkesworth, C.J., Paterson, B.A., Foster, G.L., Kinny, P.D., Whitehouse, M.J., Maas, R. & EIMF (2006a) Exploring the plutonic-volcanic link: a zircon U-Pb, Lu-Hf and O isotope study of paired volcanic and granitic units from southeastern Australia. *Transactions of the Royal Society of Edinburgh-Earth Sciences* **97**, 337-355.

Kemp, A.I.S., Hawkesworth, C.J., Paterson, B.A. & Kinny, P.D. (2006b). Episodic growth of the Gondwana supercontinent from hafnium and oxygen isotopes in zircon. *Nature* **439**, 580-583.

Kemp, A.I.S., Hawkesworth, C.J., Collins, W.J., Gray, C.M., Blevin, P.L. & EIMF (2009) Isotopic evidence for rapid continental growth in an extensional accretionary orogen: The Tasmanides, eastern Australia. *Earth and Planetary Science Letters* **284**, 455-466.

Kinny, P.D. & Maas, R. (2003). *Lu-Hf and Sm-Nd isotope systems in zircon*. In: Hanchar J.M. & Hoskin P.W.O. (ed) Zircon, vol 53. pp 327-341.

Kirsch, M., Keppie, J.D., Murphy, B.J. & Solari, L.A. (2012), Permian–Carboniferous arc magmatism and basin evolution along the western margin of Pangea: Geochemical and geochronological evidence from the eastern Acatlán Complex, southern Mexico. *Geological Society of America Bulletin* **124**, 1607-1628.

Klemperer, S.L. & Matthews, D.H. (1987). Iapetus Suture Located beneath the North-Sea by Birps Deep Seismic-Reflection Profiling. *Geology* **15**, 195-198.

Klemperer, S.L., Ryan, P.D. & Snyder, D.B. (1991). A deep seismic-reflection transect across the Irish Caledonides. *Journal of the Geological Society* **148**, 149-164.

Kneller, B.C. (1991). A Foreland Basin on the Southern Margin of Iapetus. *Journal of the Geological Society* **148**, 207-210.

Lackey, J.S., Valley, J.W. & Saleeby, J.B. (2005). Supracrustal input to magmas in the deep crust of Sierra Nevada batholith: Evidence from high- δ^{18}O zircon. *Earth and Planetary Science Letters* **235**, 315-330.

Lee, M.R., Waldron, K.A. & Parsons, I. (1995). Exsolution and alteration microtextures in alkali feldspar phenocrysts from the Shap granite. *Mineralogical Magazine* **59**, 63-78.

Leggett, J.K., McKerrow, W.S. & Soper, N.J. (1983). A model for the crustal evolution of Southern Scotland. *Tectonics* **2**, 187-210.

Lintern, B.C., Barnes, R.P. & Stone, P. (1992). Discussion on the Silurian and Early Devonian sinistral deformation of the Ratagain Granite, Scotland: constraints on the age of Caledonian movements on the Great Glen system. *Journal of the Geological Society* **149**, 858-858.

Ludwig, K.R. (2003). Isoplot 3.00. Berkeley Geochronology Center Special Publication 4.

Marschall, H.R., Hawkesworth, C.J., Storey, C.D., Dhuime, B., Leat, P.T., Meyer, H-P. & Tamm-Buckle, S. (2010). The Annandagstoppane Granite, East Antarctica: Evidence for Archaean Intracrustal Recycling in the Kaapvaal-Grunehogna Craton from Zircon O and Hf Isotopes. *Journal of Petrology* **51**, 2277-2301.

McCulloch, M.T. & Chappell, B.W. (1982). Nd isotopic characteristics of Peraluminous and Metaluminous granites. *Earth and Planetary Science Letters* **58**, 51-64.

Miles, A.J., Graham, C.M., Hawkesworth, C.J., Gillespie, M.R. & Hinton, R.W. (2013) Evidence for distinct stages of magma history recorded by the compositions of accessory apatite and zircon. *Contributions to Mineralogy and Petrology* **166**, 1-19.

Murphy, J.B., Strachan, R.A., Nance, R.D., Parker, K.D. & Fowler, M.B. (2000) Proto-Avalonia: A 1.2-1.0 Ga tectonothermal event and constraints for the evolution of Rodinia. *Geology* **28**, 1071-1074.

Nance, R.D., Murphy, J.B., Strachan, R.A., Duncan Keppie, J., Gutierrez-Alonso, G., Fernandez-Suarez, J., Quesada, C., Linnemann, U., D'Lemos, R. & Pisarevsky, S.A. (2008). *Neoproterozoic-early Palaeozoic tectonostratigraphy and palaeogeography of the peri-Gondwanan terranes: Amazonian v. West African connections*. In: Ennih NLJP (ed) Boundaries of the West African Craton, vol 297. pp 345-383.

Nance, R.D. & Murphy, J.B. (1996). *Basement isotopic signatures and Neoproterozoic paleogeography of Avalonian–Cadomian and related terranes in the circum-North Atlantic*. In: Nance, R.D., Thompson, M.A (ed) Avalonian and Related Peri-Gondwanan Terranes of the Circum-North Atlantic, vol 304. Geological Society of America, Special Papers, pp 333-346.

Neilson, J.C., Kokelaar, B.P. & Crowley, Q.G. (2009). Timing, relations and cause of plutonic and volcanic activity of the Siluro-Devonian post-collision magmatic episode in the Grampian Terrane, Scotland. *Journal of the Geological Society* **166**, 545-561.

O'Nions, R.K., Hamilton, P.J. & Hooker, P.J. (1983). A Nd isotope investigation of sediments related to crustal development in the British Isles. *Earth and Planetary Science Letters* **63**, 229-240.

Oliver, G.J.H., Wilde, S.A. & Wan, Y.S. (2008). Geochronology and geodynamics of Scottish granitoids from the late Neoproterozoic break-up of Rodinia to Palaeozoic collision. *Journal of the Geological Society* **165**, 661-674.

O'Reilly, B.M., Hauser, F. & Readman, P.W. (2012). The fine-scale seismic structure of the upper lithosphere within accreted Caledonian lithosphere: implications for the origins of the 'Newer Granites'. *Journal of the Geological Society* **169**, 561-573.

Parrish, R. & Noble, S.R. (2003). *Zircon U-Pb geochronology by isotope dilution - thermal ionisation mass spectrometry (ID-TIMS)* In: Hanchar J.M. & Hoskin P.W.O. (ed) Zircon, vol 53. pp 183-213.

Parslow, G.R. (1968). The physical and structural features of the Cairnsmore of Fleet granite and its aureole. *Scottish Journal of Geology* **9**, 91-108.

Parslow, GR & Randall, B.A.O. (1973). A gravity survey of the Cairnsmore of Fleet granite and its environs. *Scottish Journal of Geology* **9**, 219-231.

Paterson, S.R. & Fowler, T.K. (1993). Re-examining pluton emplacement process. *Journal of Structural Geology* **15**, 191-206.

Peck, W.H., Valley, J.W., Wilde, S.A. & Graham, C.M. (2001). *Oxygen isotope ratios and rare earth elements in 3.3 to 4.4 Ga zircons*: Ion microprobe evidence for high $\delta^{18}O$ continental crust and oceans in the Early Archean. *Geochimica Et Cosmochimica Acta* **65**, 4215-4229.

Phillips, E.R., Barnes, R.P., Boland, M.P., Fortey, N.J., McMillan, A.A. (1995). The Moniaive Shear Zone: a major zone of sinistral strike-slip deformation in the Southern Uplands of Scotland. *Scottish Journal of Geology* **3**1, 139-149.

Pidgeon, R.T. & Aftalion, M. (1978). *Cogenetic and inherited zircon U-Pb systems in granites: Palaeozoic granites of Scotland and England*. In Bowes, D.R., Leake, B.E., Crustal evolution in northwestern Britain and adjacent regeions. *Geological Journal Special Issue* 183-220.

Read, H. (1961). Aspects of the Caledonian magmatism in Scotland. *Proceedings of the Liverpool and Manchester Geological Society* **2**, 653-683.

Roberts, N. (2012). Increased loss of continental crust during supercontinent amalgamation. *Gondwana Research* **21**, 994-1000.

Rock, N.M.S., Gaskarth, J.W. & Rundle, C.C. (1986). Late Caledonian Dyke-Swarms in Southern Scotland - a Regional Zone of Primitive K-Rich Lamprophyres and Associated Vents. *Journal of Geology* **94**, 505-522.

Scherer, E., Munker, C. & Mezger, K. (2001). Calibration of the lutetium-hafnium clock. *Science* **293**, 683-687.

Segal, I., Halicz, L. & Platzner, I.T. (2003). Accurate isotope ratio measurements of ytterbium by multi-collector inductively coupled plasma mass spectrometry applying erbium and hafnium in an improved double external normalisation procedure. *Journal of Analytical Atomic Spectrometry* **18**, 1217-1223.

Sláma, J. et al. (2008) A new reference material for U-Pb and Hf isotopic microanalysis. *Chemical Geology* **249**, 1-35.

Soper, N.J. (1986). The Newer Granite Problem - a Geotectonic View. *Geological Magazine* **123**, 227-236.

Soper, N.J. (1987). The Ordovician Batholith of the English Lake District. *Geological Magazine* **124**, 481-482.

Soper, N.J. & Kneller, B.C. (1990). Cleaved microgranite dykes of the Shap swarm in the Silurian of NW England. *Geological Journal* **25**, 161-170.

Soper, N.J., Strachan, R.A., Holdsworth, R.E., Gayer, R.A. & Greiling, R.O. (1992). Sinistral transpression and the Silurian closure of Iapetus. *Journal of the Geological Society* **149**, 871-880.

Soper, N.J. & Woodcock, N.H. (2003). The lost Lower Old Red Sandstone of England and Wales: a record of post-Iapetan flexure or Early Devonian transtension? *Geological Magazine* **140**, 627-647.

Stephens, W.E. (1988). *Granitoid plutonism in the Caledonian orogen of Europe*. In: Harris, A., Fettes, D.J. (ed) The Caledonian-Appalachian Orogen, vol 38. Geological Society of London, Special Publication, pp 389-403.

Stephens, W.E. & Halliday, A.N. (1980), Discontinuities in the composition surface of a zoned pluton, Criffel, Scotland. *Geological Society of America Bulletin* **91**, 165-170.

Stephens, W.E. & Halliday, A.N. (1984). Geochemical contrasts between late Caledonian granitoid plutons of northern, central and southern Scotland. *Transactions of the Royal Society of Edinburgh-Earth Sciences* **75**, 259-273.

Stephens, W.E., Whitley, J. E., Thirwall, M.F. & Halliday, A. N. (1985). The Criffell zoned pluton: correlated behaviour of rare earth element abundances with isotopic systems. *Contributions to Mineralogy and Petrology* **89**, 226-238.

Stephenson, D.B. (1999). Caledonian Igneous Rocks of Great Britain, vol. Joint Nature Conservation Committee, pp 1-648

Stone, P. and Evans, J.A. (1995). Nd-isotope study of provenance patterns across the Iapetus Suture. *Geological Magazine*. **132,** 571-580.

Stone, P. & Evans, J.A. (1997). A comparison of the Skiddaw and Manx groups (English Lake District and Isle of Man) using neodymium isotopes. *Proceedings of the Yorkshire Geological Society* **51**, 343-347.

Teyssier, C., Tikoff, B. & Markley, M. (1995). Oblique plate motions and continental tectonics. *Geology* **23**, 447-450.

Thirlwall, M.F. (1981). Implications for Caledonian Plate Tectonic Models of Chemical-Data from Volcanic-Rocks of the British Old Red Sandstone. *Journal of the Geological Society* **138**, 123-138.

Thirlwall, M.F. (1982). Systematic variations in chemistry and Nd and Sr isotopes across a Caledonian calc-alkaline volcanic arc - implications for source materials. *Earth and Planetary Science Letters* **58**, 27-50.

Thirlwall, M.F. (1983). Isotope geochemistry and origin of calc alkaline lavas from a Caledonian continental margin volcanic arc. *Journal of Volcanology and Geothermal Research* **18**, 589-631.

Thirlwall, M.F. (1986). Lead isotope evidence for the nature of the mantle beneath Caledonian Scotland. *Earth and Planetary Science Letters* **80**, 55-70.

Thirlwall, M.F. (1989). Movement on proposed terrane boundaries in northern Britain: constraints from Ordovician-Devonian igneous rocks. *Journal of the Geological Society, London* **146**, 373-376.

Thomas, L.J., Harmon, R.S. & Oliver, G.J.H. (1985). Stable isotope composition of alteration fluids in low-grade Lower Palaeozoic Rocks, English Lake District. *Mineralogical Magazine* **49**, 425-434.

Thorogood, E.J. (1990). Provenance of the pre-Devonian sediments of England and Wales: Sm-Nd isotopic evidence. *Journal of the Geological Society* **147**, 591-594.

Tikoff, B. & Teyssier, C. (1992). Crustal-scale, en echelon "P-shear" tensional bridges: A possible solution to the batholithic room problem. *Geology* **20**, 927-930.

Valley, J.W., Chiarenzelli, J.R. & McLelland, J.M. (1994). Oxygen-Isotope Geochemistry of Zircon. *Earth and Planetary Science Letters* **126**, 187-206.

Valley, J.W., Kinny, P.D., Schulze, D.J., Spicuzza, M.J. (1998). Zircon megacrysts from kimberlite: oxygen isotope variability among mantle melts. *Contributions to Mineralogy and Petrology* **133**, 1-11.

Valley, J.W., Lackey, J.S., Cavosie, A.J., Clechenko, C.C., Spicuzza, M.J., Basei, M.A.S., Bindeman, I.N., Ferreira, V.P., Sial, A.N., King, E.M., Peck, W.H., Sinha A.K., Wei, C.S. (2005) 4.4 billion years of crustal maturation: oxygen isotope ratios of magmatic zircon. *Contributions to Mineralogy and Petrology* **150**, 561-580.

Vervoort, J.D., Patchett, P.J., Blichert-Toft, J. & Albarede, F. (1999) Relationships between Lu-Hf and Sm-Nd isotopic systems in the global sedimentary system. *Earth and Planetary Science Letters* **168**, 79-99.

Vervoort, J.D., Patchett, P.J., Söderlund, U. & Baker, M. (2004). The isotopic composition of Yb and the precise and accurate determination of Lu concentrations and Lu/Hf ratios by isotope dilution using MC-ICPMS. *Geochemistry, Geophysics, Geosystems.*

Waldron, J.W.F., Floyd, J.D., Simonetti, A. & Heaman, L.M. (2008). Ancient Laurentian detrital zircon in the closing Iapetus Ocean, Southern Uplands terrane, Scotland. *Geology* **36**, 527-530.

Wadge, A.J., Gale, N.H., Beckinsale, R.D. & Rundle, C.C. (1978). A Rb-Sr isochron age for the Shap Granite. *Proceedings of the Yorkshire Geological Society* **42**, 297-305.

Weinberg, R.F., Sial, A. & Mariano, G. (2004). Close spatial relationship between plutons and shear zones. *Geology* **32**, 377-380.

Wiedenbeck, M., Allé, P., Corfu, F., Griffin, W.L., Meier, M., Oberli, F., Vonquadt, A., Roddick, J.C. & Speigel, W. (1995). 3 Natural zircon standards for U-Th-Pb, Lu-Hf, trace elements and REE analyses. *Geostandards Newsletter* **19**, 1-23.

Wiedenbeck, M., Hanchar, J.M., Peck, W.H., Sylvester, P., Valley, J., Whitehouse, M., Kronz, A., Morishita, Y., Nasdala, L., Fiebig, J., Franchi, I., Girard, J.P., Greenwood, R.C., Hinton, R., Kita, N., Mason, P.R.D., Norman, M., Ogasawara, M., Piccoli, R., Rhede, D., Satoh, H., Schulz-Dobrick, B., Skar, O., Spicuzza, M.J., Terada, K., Tindle, A., Togashi, S., Vennemann, T., Xie, Q. & Zheng, Y.F. (2004). Further characterisation of the 91500 zircon crystal. *Geostandards and Geoanalytical Research* **28**, 9-39.

Woodhead, J.D., and Hergt, J.M. (2005) . A preliminary appraisal of seven natural zircon reference materials for in situ Hf isotope determination. *Geostandards and Geoanalytical Research* **29**, 183-195.

Zindler, A. & Hart, S. (1986). Chemical Geodynamics. *Annual Review of Earth and Planetary Sciences* **14**, 493-571.

Figures

Fig. 1 Modified map of late Caledonian (early Devonian) plutonic and volcanic rocks in the northern United Kingdom, modified from Highton (1999). Plutons are classified according to the geochemical parameters outlined by Read (1961), Stephens & Halliday (1980) and Stone & Evans, 1997.

Fig. 2 Simplified geological maps of the Criffell (a), Fleet (b) and Shap (c) plutons. Zone colouration reflects approximate silica content, with darker colours indicative of lower SiO_2. Zone mineralogy in the Criffell pluton is as follows: 1) clinopyroxene-biotite-hornblende granodiorite; 2) biotite-hornblende granodiorite; 3) biotite granite; 4) biotite-muscovite granite 5) muscovite-biotite granite. Zone mineralogy in the Fleet pluton is as follows: 1) coarse grained biotite granite; 2) coarse-grained biotite-muscovite granite; 3) fine-grained biotite-muscovite granite. Minerals listed in order of increasing modal abundance. Black circles denote sample sites with the following sample numbers: Criffell: Zone 1 – AM0917, Zone 2 – AM0918, Zone 3 – AM0921, Zone 4 – AM0922, Fleet: Zone 1 – AM0933, Zone 2 – AM0934, Zone 3 – AM0935, Shap: Zone 1 – westerly-most point: AM0923, Zone 2 – easterly-most point: AM0932.

Fig. 3 Aluminium saturation indices for whole-rock data from the Criffell, Fleet and Shap plutons. Whole-rock data are from Stephens and Halliday (1980), Stephens *et al.* (1985) and Miles *et al.* (2013). Criffell samples are distinguished by zone (see key) and show a trend from outer, more primitive metaluminous granodiorites to more evolved peraluminous inner granites.

Fig. 4 Representative photomicrographs of the Criffell, Fleet and Shap ganitoids. (a) Zone 1 granodiorite (Criffell); (b) Zone 5 granite (Criffell); (c) Zone 2 granite (Fleet); (d) Zone 3 granite (Fleet); (e) Stage 2 granite (Shap). Abbreviations are as follows: Ap – apatite, Bt – biotite, Cpx – clinopyroxene, Hb – hornblende, K-Spar – Potassium feldspar, Mag – magnetite, Mu – muscovite, Plag – plagioclase, Qtz – quartz, Sp – sphene (titanite).

Fig. 5 CL images of a representative selection of zircon crystals from the Criffell pluton. Concentric zoning is evident in most crystals. Two crystals show laser and SIMS analysis pits with their analytical results. U-Pb pits for samples 21_39 and 22_39 are located beneath the laser pits outlined. Darker discordant and potentially younger overgrowths are evident around grains 17_56, 21_39, 22_52 and 22_39.

Fig. 6 Pb-Pb isotope diagram modified from Thirlwall (1989) showing the Pb isotope compositions of the TSS plutons, Skiddaw Group sediments (Thomas *et al*. 1985; Stone & Evans 1997), Southern Uplands sediments (Stone & Evans 1995), Borrowdale Volcanic Group (BVG) (Thirlwall, 1986) and depleted mantle (Zindler & Hart, 1986). All plutons extend to more radiogenic $^{207}Pb/^{204}Pb$ compositions than the Southern Uplands sediments into which they are intruded. The Fleet pluton in particular also extends to more radiogenic compositions than the Skiddaw sediments, and implies that a further upper crustal component was involved, potentially unexposed Avalonian basement. Numbers in brackets refer to the number of analyses. μ values refer to different the ratios of $^{238}U/^{204}Pb$.

Fig. 7 Cumulative $\delta^{18}O$(Zrc) probability-histograms for zircon crystals from zones 1 to 4 of the Criffell pluton and zones 1 to 3 of the Fleet pluton. Outer zones of both plutons show more homogeneity in composition than inner, more silicic zones. Bin widths of histograms determined by 1 SD analytical errors; error bars are for 2 SD analytical errors. Mantle zircon composition from Valley *et al.* (1998).

Fig. 8 Cumulative $\delta^{18}O$(Zrc) probability-histograms for the Shap granite. Bin widths of histograms are 1 SD; error bars are for 2 SD analytical errors. Mantle zircon composition from Valley *et al.* (1998).

Fig. 9 Cumulative $\delta^{18}O$(Zrc) probability-histograms for enclaves and their host granitoids from the Criffell (a and b) and Shap (c and d) plutons. Bin widths are for 1 SD analytical errors. The mean and 2 SD values for enclave and host populations are indicated. Mantle zircon composition from Valley *et al.* (1998).

Fig. 10 Tectono-stratigraphic framework for Britain during Silurian-Devonian times (after Soper & Woodcock, 2003 and Brown *et al.*, 2008). New zircon U-Pb ages are used to re-position the TSS plutons into an independently inferred transtensional tectonic regime, co-incident with the deposition of sediments in transtensional basins and the intrusion of the regional swarm of lamprophyre dykes. F(I) and F(II) refer to the two stages of pluton emplacement in the Fleet pluton.

Fig. 11 εHf_t vs. $\delta^{18}O$ of zircons from the Criffell, Fleet and Shap plutons, with the estimated average compositions (with 1 SD) of potential endmembers. The composition of Eastern Avalonian basement is estimated from recalculated Nd isotope compositions (using the Nd-Hf correlation from Vervoort *et al*. 1999) using data from Murphy *et al*. (2000). No oxygen isotope data for Avalonian basement are available. Mixing with Skiddaw Group (or similar) sediments is proposed to generate the vertical arrays of compositions, marked with 10% increments of sedimentary contaminant. Other source rock compositions are: Depleted mantle: Vervoort *et al.* (1999); Avalonian basement: Murphy *et al*. (2000); Skiddaw Group sediments: Stone & Evans (1997); Thomas *et al.* (1985). Oxygen isotope compositions for the Skiddaw Group have been re-calculated as equilibrium zircon compositions using the whole-rock-zircon equilibrium relationship outlined by Lackey *et al*. (2005).

Fig. 12 Model age calculations for the TSS plutons calculated using the ‘new crust’ reference line of Dhuime *et al*. (2011). A Lu/Hf ratio of 0.015 has been used assuming silicic crust. Model age estimates are youngest for the Criffell pluton and increase in the Fleet and Shap plutons and lie within the range of model ages estimated for Avalonian basment (between horizontal arrows) (Murphy *et al*. 2000) re-calculated using the ‘new crust’ Nd reference line (see text). Zircon crystallization ages (Zrc. cryst. age) are shown by the vertical arrow.

Fig. 13 Cross-section of the Iapetus Suture based on the reconstruction of Brown *et al*. (2008) along the UK Geotraverse North line at the present day showing proposed Hf, O and Pb isotope compositions of granitoids and possible magma sources. Horizontal scale is the same in all plots. Avalonian crust is shown underthrusting the Laurentian margin with proposed hot zones at depths of > 11 km within the underthrust Avalonian crust (positions beneath the suture are unconstrained). P1 and P2 represent prominent seismic reflectors interpreted as either Iapetus oceanic crust or imbricated basement and sedimentary cover (see text). Vertical, curved arrows represent ascent of lamprophyric melts into the crust and their possible role as contributing melts and heat sources in the genesis of the TSS. Abbreviations are: GHT – Grampian Highland Terrane; HBF – Highland Boundary Fault; SUF – Southern Uplands Fault; OBF – Orlock Bridge Fault; SUS – Southern Uplands Sediments; IS – Iapetus Suture; WFB – Windermere Flexural Basin; Skid. – Skiddaw Group sediments; Av. – Avalonia; zrc – zircon compositions. Granitoid O and Hf (recalculated at 410 Ma) isotope compositions are those measured in this study in zircons from the Criffell, Fleet and Shap plutons. Pb isotope data are from Thirlwall (1989). Depleted mantle Pb isotope compositions around the Iapetus Suture at 410 Ma are from Frost & O'Nions (1985). Hf compositions (recalculated at 410 Ma) are estimated from published Nd data using the Nd-Hf relationship of Vervoort *et al.* (1999). Mantle oxygen isotope compositions are from Valley *et al.* (1998). Other data sources include: Stone & Evans (1997), Thomas *et al*. (1985), Thirlwall (1986), O'Nions *et al*. (1983), Halliday *et al*. (1980), Murphy *et al*. (2000).

Table 1 Summary of oxygen, Hf and U-Pb data for zircon

Pluton	Sample	SiO_2 (wt%)	$\delta^{18}O$(Zrc) ‰*	±2σ	n	εHf_t(Zrc)†	±2σ	n	$^{206}Pb/^{238}U$ (Ma)	±2σ	n
Criffell	Zone 1 (0917)	63.9	5.8	0.8	13	+2.9	0.7	10	408	14	9
	Zone 2 (0918)	66.0	5.9	0.9	13	+3.8	0.6	10	409	14	9
	Zone 3 (0921)	69.5	6.5	1.0	21	+3.7	0.8	10	414	10	7
	Zone 4 (0922)	68.8	7.2	1.4	28	+3.1	0.5	10	412	5	4
	Enc. Zone 1 (0917E)		6.3	0.5	15	+3.1	0.7	10	411	6	10
	Enc. Zone 2 (0918E)		6.2	0.4	15	+3.9	0.7	10	420	8	6
Fleet	Zone 1 (0933)	68.8	6.8	0.8	15	+0.7	1.2	10	410	6	4
	Zone 2 (0934)	71.2	7.1	1.5	15	+0.1	1.7	10	386	8	7
	Zone 3 (0935)	73.8	6.4	1.7	10	+1.2	2.4	5	391	8	3
Shap	Zone 1 (0923)	67.0	7.9	0.5	25	-0.2	0.7	10	417	13	7
	Zone 2 (0932)	69.1	7.6	0.4	20	-0.4	1.2	10	414	3	4
	Enc. Zone1 (0925)		7.7	0.6	24	-0.2	0.7	9	418	8	7
	Enc. Zone 2 (0926)	59.7	7.8	0.8	25				417	6	5

Enc. = enclave. * = 2 SD analytical errors vary from session to session but are generally between 0.3‰ and 0.6‰. † = 2 SD analytical error of ±0.8εHf units

Figure 1

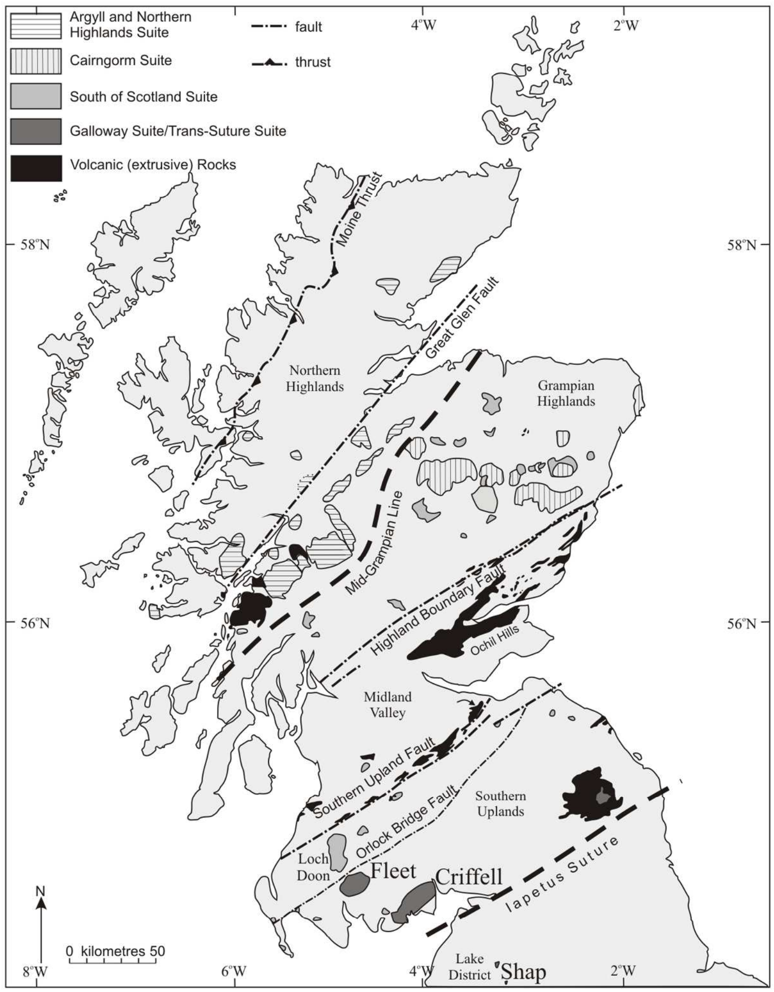

132x182mm (300 x 300 DPI)

Figure 2

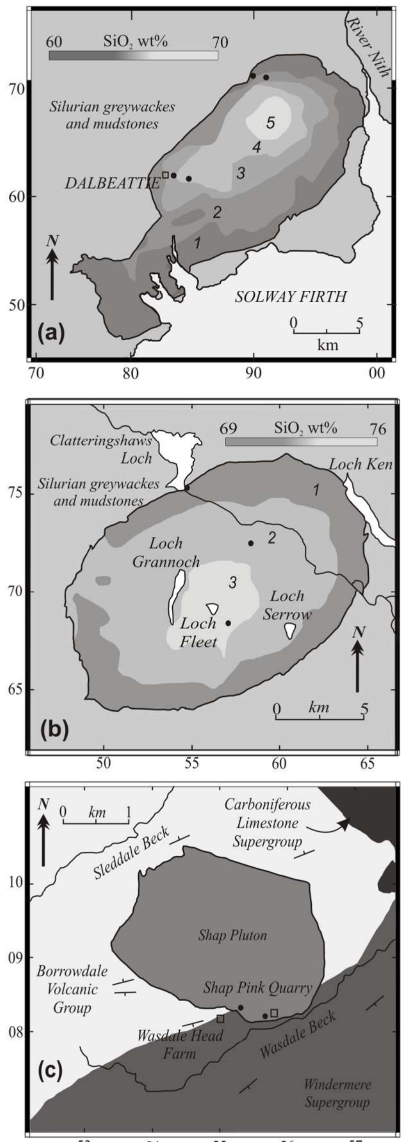

112x203mm (300 x 300 DPI)

Figure 3

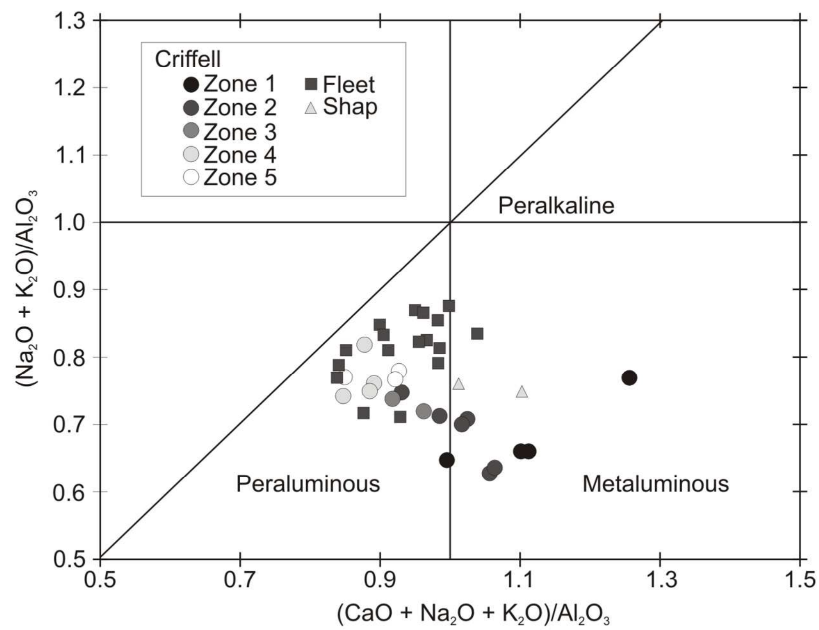

156x128mm (300 x 300 DPI)

Figure 4

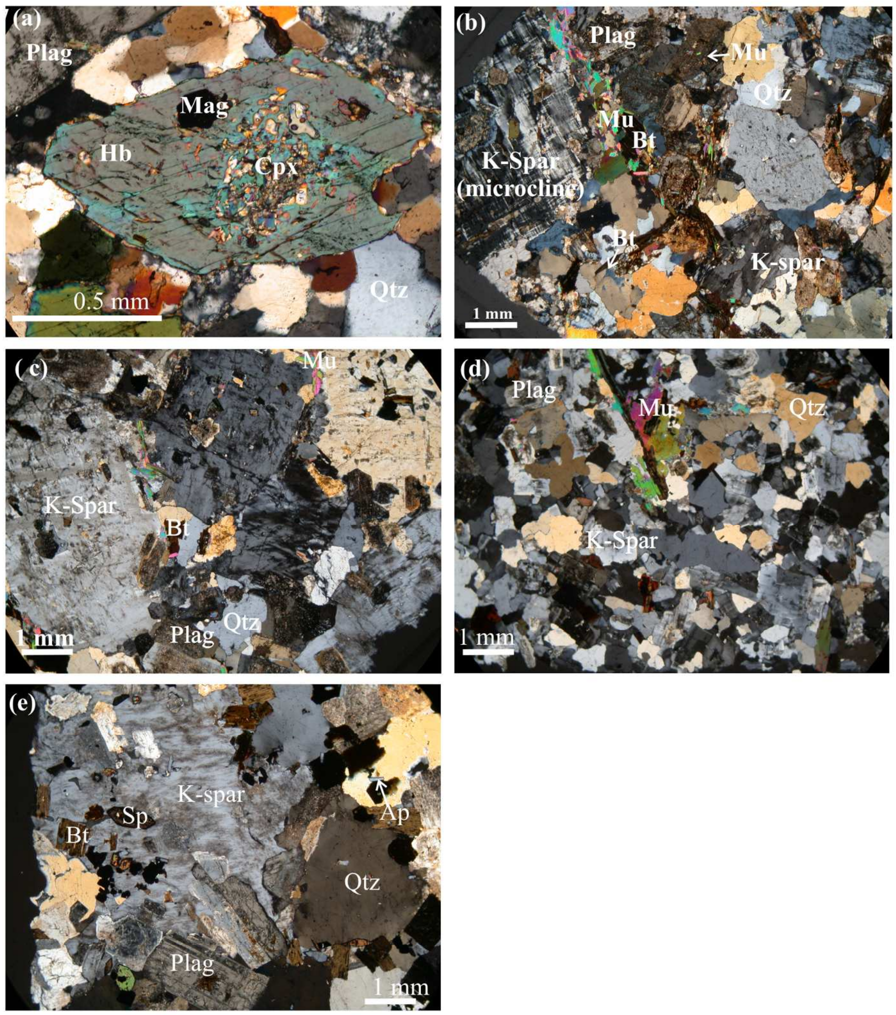

170x196mm (300 x 300 DPI)

Figure 5

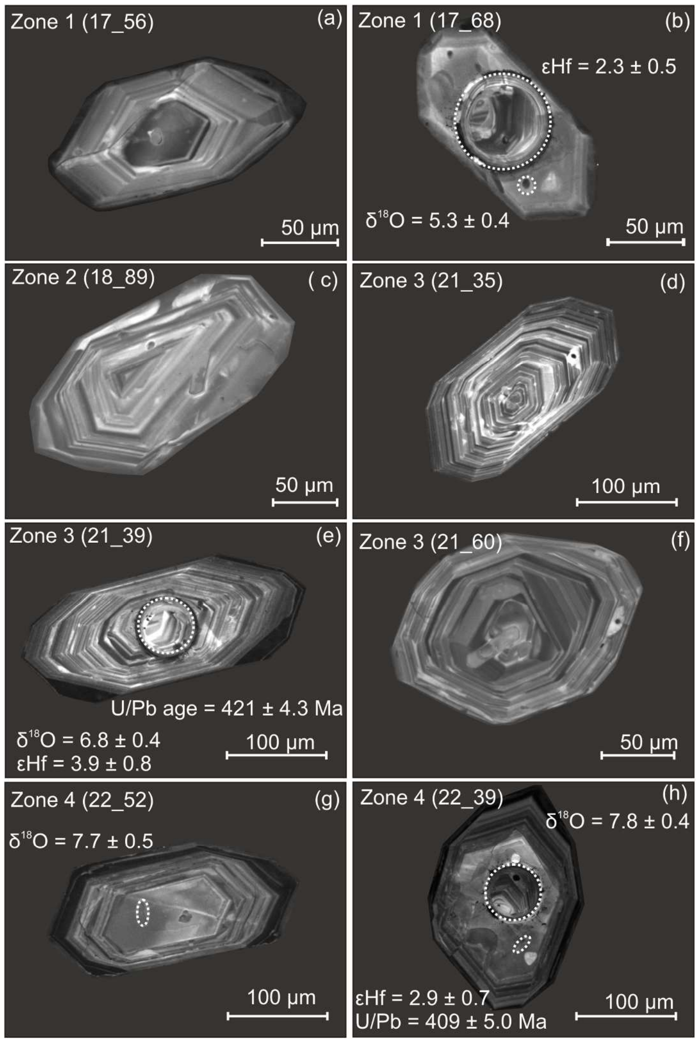

166x243mm (300 x 300 DPI)

Figure 6

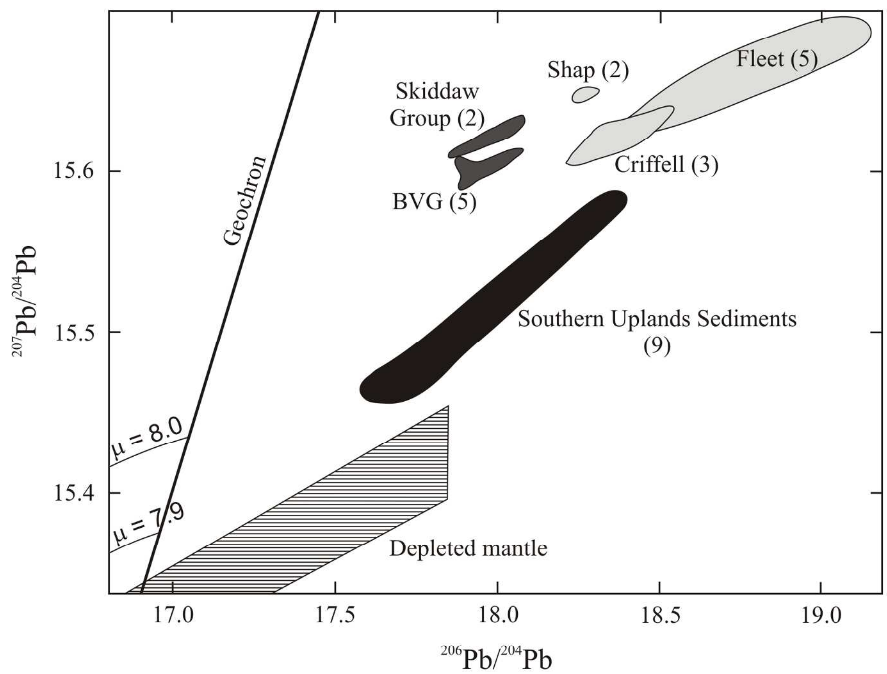

171x155mm (300 x 300 DPI)

Figure 7

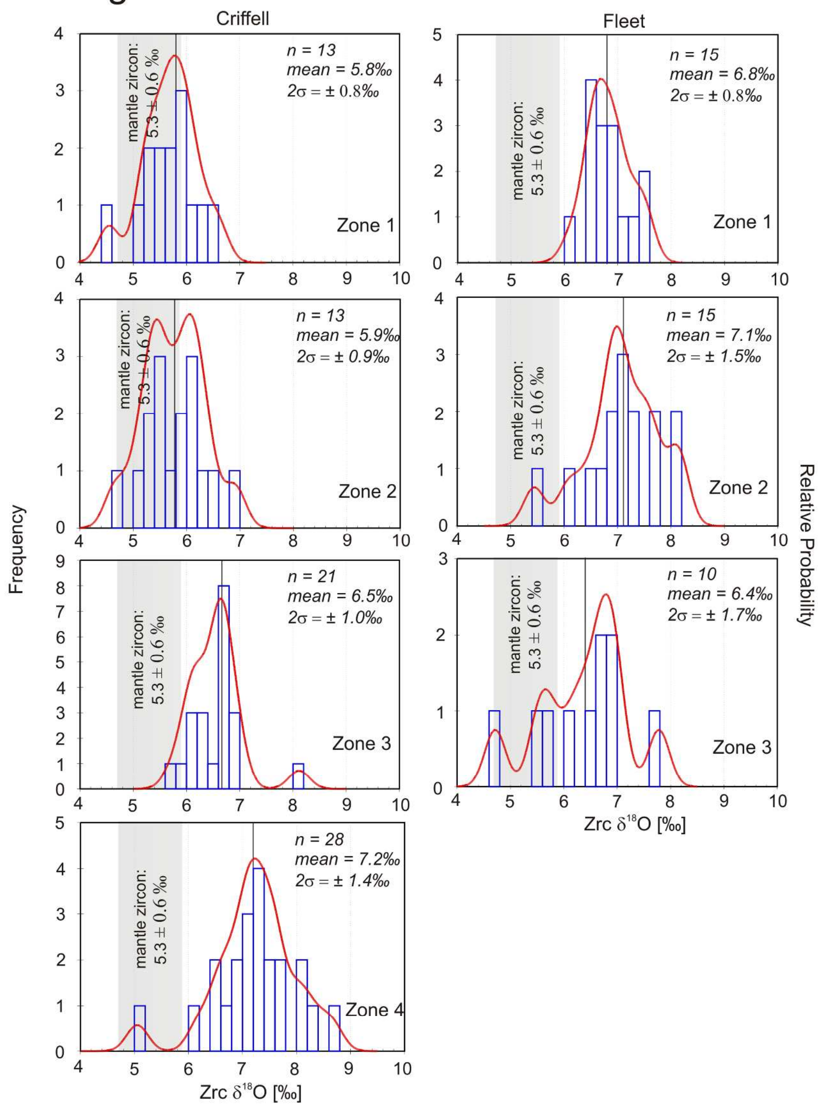

188x266mm (300 x 300 DPI)

Figure 8

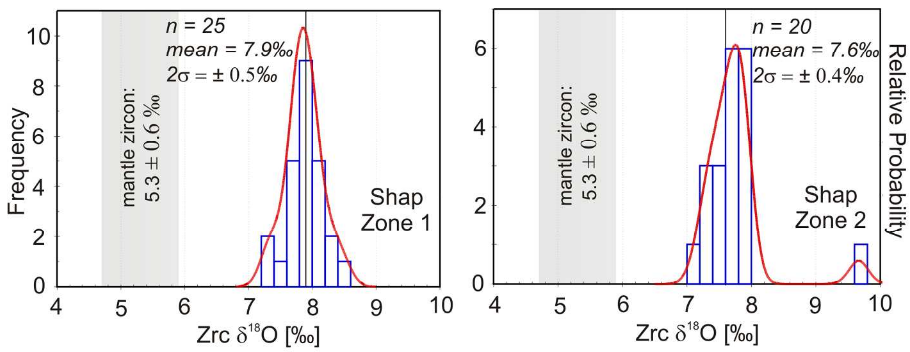

184x99mm (300 x 300 DPI)

Figure 9

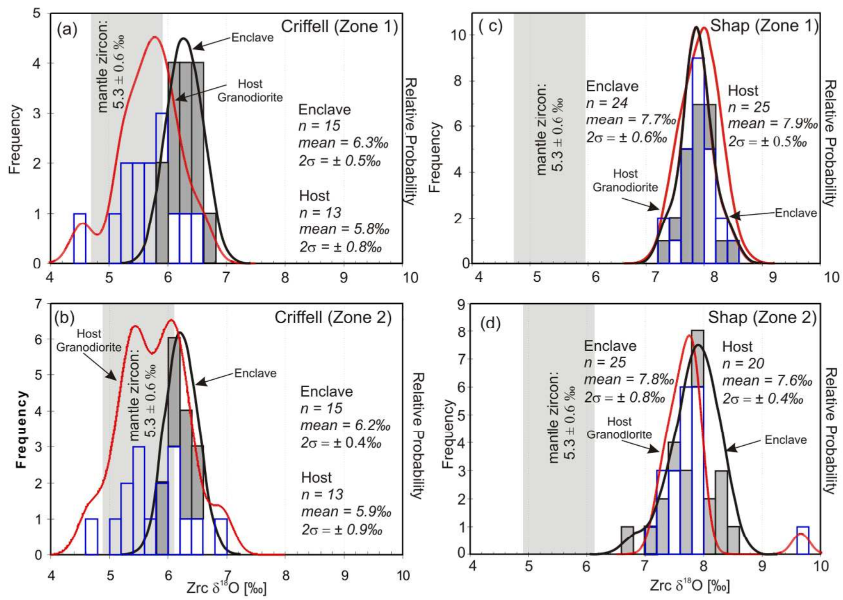

207x151mm (300 x 300 DPI)

Figure 10

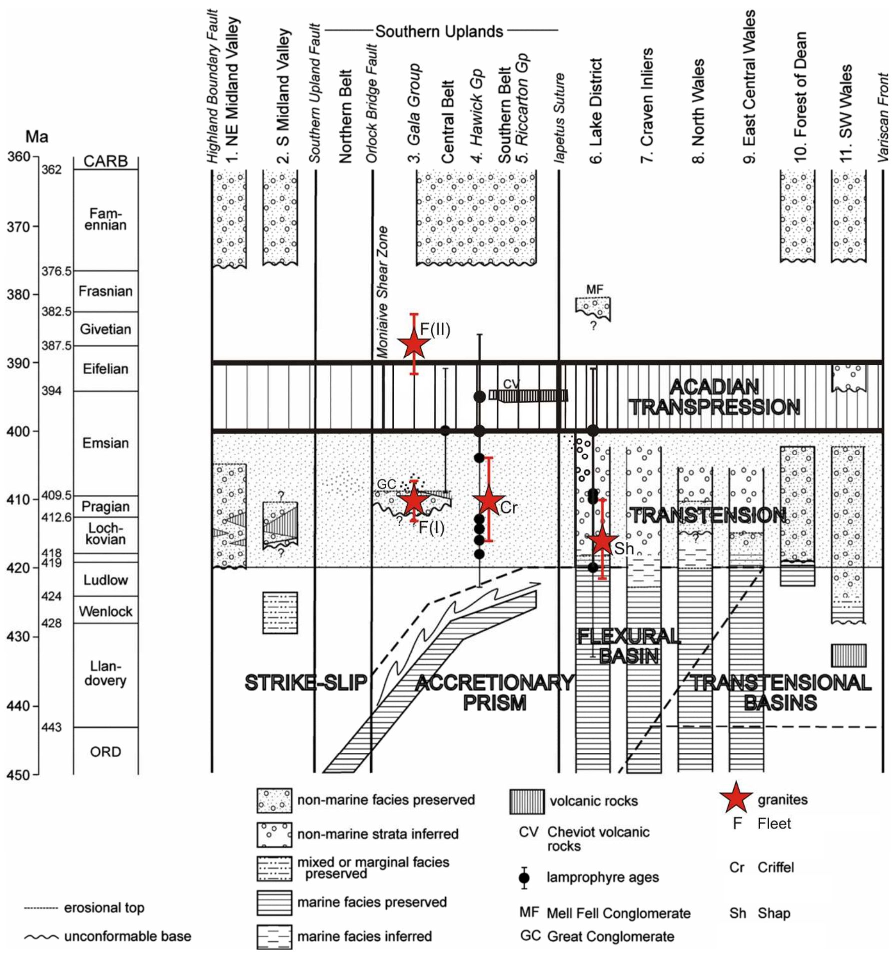

188x224mm (300 x 300 DPI)

Figure 11

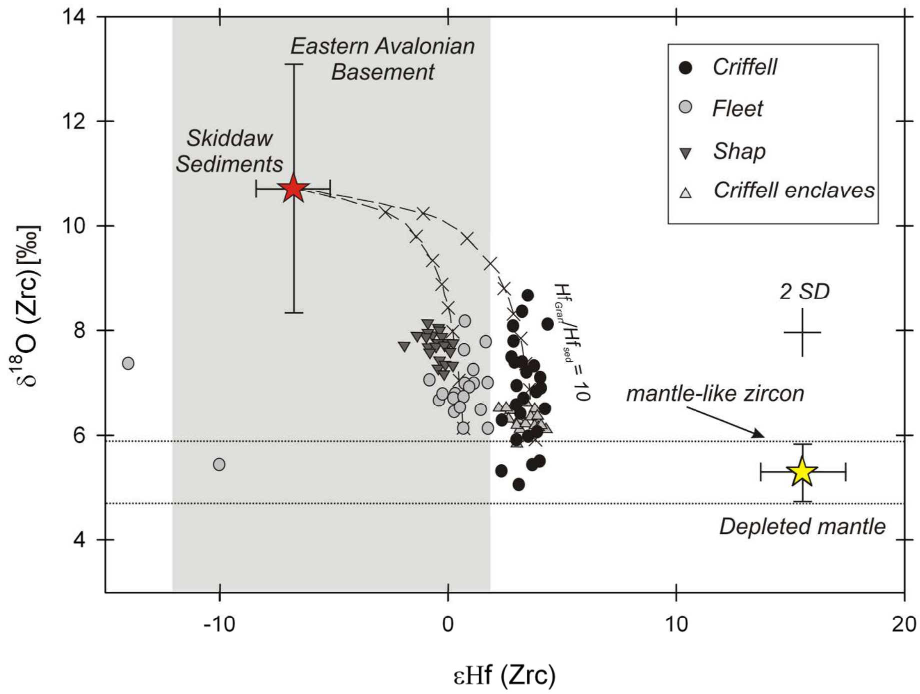

184x157mm (300 x 300 DPI)

Figure 12

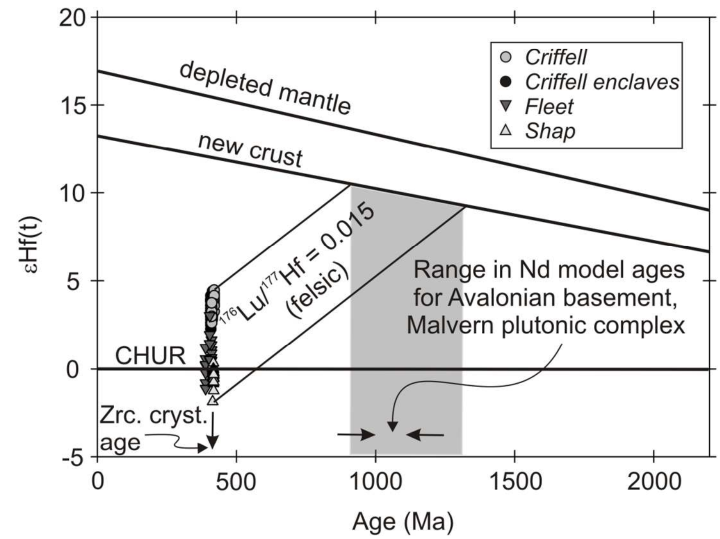

161x127mm (300 x 300 DPI)

Figure 13

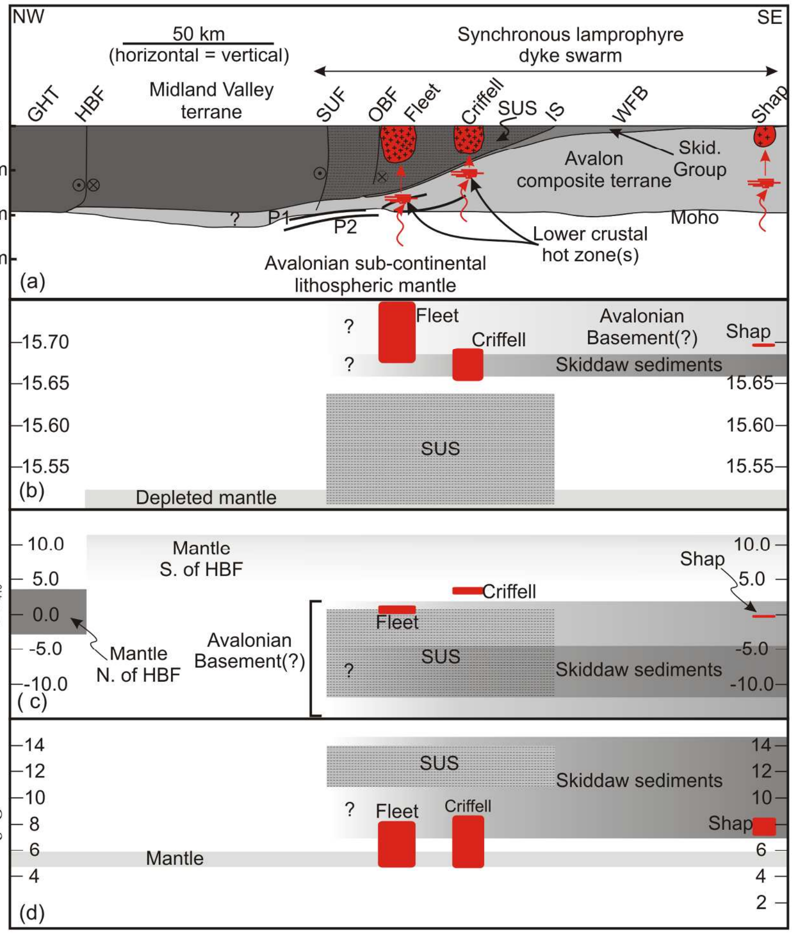

200x200mm (300 x 300 DPI)